Splash, pop, sizzle: Information processing with phononic computing

Cite as: AIP Advances **5**, 053302 (2015); https://doi.org/10.1063/1.4919584
Submitted: 31 January 2015 • Accepted: 21 April 2015 • Published Online: 28 April 2015

Sophia R. Sklan

Splash, pop, sizzle: Information processing with phononic computing

Sophia R. Sklan
Department of Physics, Massachusetts Institute of Technology, Cambridge, Massachusetts 02139, USA

(Received 31 January 2015; accepted 21 April 2015; published online 28 April 2015)

Phonons, the quanta of mechanical vibration, are important to the transport of heat and sound in solid materials. Recent advances in the fundamental control of phonons (phononics) have brought into prominence the potential role of phonons in information processing. In this review, the many directions of realizing phononic computing and information processing are examined. Given the relative similarity of vibrational transport at different length scales, the related fields of acoustic, phononic, and thermal information processing are all included, as are quantum and classical computer implementations. Connections are made between the fundamental questions in phonon transport and phononic control and the device level approach to diodes, transistors, memory, and logic. [http://dx.doi.org/10.1063/1.4919584]

Historically, information processing was handled mechanically. The earliest known calculator, Antikythera mechanism,[1] was purely mechanical. That technology was then lost and independently created by Pascal[2] and Abu Rayhan al-Biruni.[3] Similarly, the earliest robots (called automaton, predating the invention of the word robot by millennia) were invented by the Greeks.[4,5] This technology was developed continuously afterwards, going from pulleys and water pressure to clockwork. The first true computer, Babbage's analytic engine[6] (a development on his original difference engine, itself an advanced mechanical calculator), was inspired by these devices. While Babbage invented the design, it was Ada Lovelace who demonstrated that it was a true computer and not merely a calculator.[7] Within a comparatively short time, however, this entire tradition of mechanical computing virtually disappeared, replaced entirely by electronic computing.

Today, however, the pressures of Moore's Law and Landauer entropy are pushing silicon-based electronic computing to its limit.[8] As such, there is increased attention on alternative methods of computation (see Table. I). Some of these, like spintronics and quantum computing, would entirely supplant electronic computing. Others, like biological or fuzzy logic computing merely have niche applications where they can outperform their electronic counterparts (in vivo computing and control systems, respectively). Still others, like mechanical computing or swarm computing, are kept on out of historical or theoretical interest. Recently, though, mechanical computing has been revived in an entirely novel form, the phononic computer. Instead of using the static configurations of a mechanical system, phononic computing relies upon the system's vibrations, or phonons. It is this new approach to computing that shall be the focus of this article. Because phononic computing is still in its earliest stages, the precise nature of the technology and its applications is still being developed. Moreover, there are a great many different approaches towards each part of the technology (diodes and transistors for logic and memory). Phonons can take the form of low frequency (Hz-MHz) acoustic and ultrasonic waves, to mid frequency (MHz-THz) hypersound, to high frequency (THz) waves (the thermal regime).[9] For each of these regimes the implementations will be slightly different. Acoustic and ultrasonic signals have sufficiently long wavelengths that there are convenient implementations for both phonons in solids and waves in gases or liquids. Hypersound is more often the domain of purely solid-state, phononic devices. THz waves are of such short wavelength that it is often easier to ignore the wave nature of these phonons and focus instead on thermal conduction from these high frequency phonons.

TABLE I. Various computing architectures or approaches and their roles, given current developments.

Role	Architecture
Dominant	Electronic
Rival	Quantum, Spintronic, Reversible
Niche	Chemical, Fuzzy Logic, Optical, Wetware
Emerging	Phononic, Swarm, BZ Wave
Historical	Ternary, Mechanical, Hydraulic
Theoretical	Hypercomputer, Black Hole

This paper will be organized as follows. Diodes, transistors, and memory will each be considered in its own section. The connection between each device and fundamental questions of phonon physics will be developed and used to organize the different approaches within each section. Logic gates and alternative approaches outside of the classical diode/transistor logic will be considered in a separate section.[10] Finally, I'll present potential future directions and applications for phononic computing.

I. DIODES

A diode is a device that displays an asymmetric transmission of two related inputs. For example, the electrical diode produces a large current for a positive voltage gradient and almost no current for a negative voltage gradient. In photonics, on the other hand, the analogue of the diode is the isolator, which has a large transmission coefficient for polarized photons along the forward direction and a small transmission coefficient for the time-reversed photons along the reverse direction (see Fig. 1). The exact nature of the relation between the two inputs has been the subject of great debate phononics. Maznev *et al.*[12] argued on the basis of the *R-T* reciprocity theorem that the comparison should be between the time-reversed output of the original input, thereby requiring a diode that breaks time-reversal symmetry or linearity. In the other school of thought, the comparison is between the reflected or inverted original input, meaning that only a breaking of reflection symmetry is necessary. Both classes of devices are potentially useful, but the first category gives a more robust definition of rectification (used in the phononic context as an asymmetry between related inputs, a definition closely related to – but not identical with – the creation of a constant output from an oscillating input). Regardless of the formulation, a diode requires the breaking of $\mathcal{P}$ (parity, or reflection) symmetry, $\mathcal{T}$ (time-reversal) symmetry, or $\mathcal{PT}$ symmetry. The question of how to break these symmetries for phonons is what will occupy us here, so I shall present each symmetry relation in turn.

A. $\mathcal{P}$ Symmetry

Extensive reviews of rectification (specifically thermal rectification $q(\Delta T)/q(-\Delta T) \neq 1$ where q is heat flux) through broken parity were recently presented in Refs. 13 and 14. There are a variety of mechanisms that can produce thermal rectification, not all of which will be discussed here. For example, the boundary between a metal and an insulator will produce rectification, as the metal will transport heat by both electrons and phonons while the insulator will only transport heat via phonons.[15] This asymmetry in the different transport channels is not a purely phononic effect, hence the exclusion, but does point to one of the two fundamental forms of thermal rectification. Thermal rectification comes from mismatch in the transport channels (phonon modes) between layers or from mismatch of the thermal conductivity's temperature dependence at each side of the boundary. While these effects are often related to each other for both inhomogeneous systems and single interfaces, one important effect of geometry is commonly observed. For a single interface, there tends to be a decrease in rectification with increasing system size (as the thermal gradient near the interface decreases), whereas for an inhomogeneous system there is no such decay (as rectification is often a local effect in this setup).

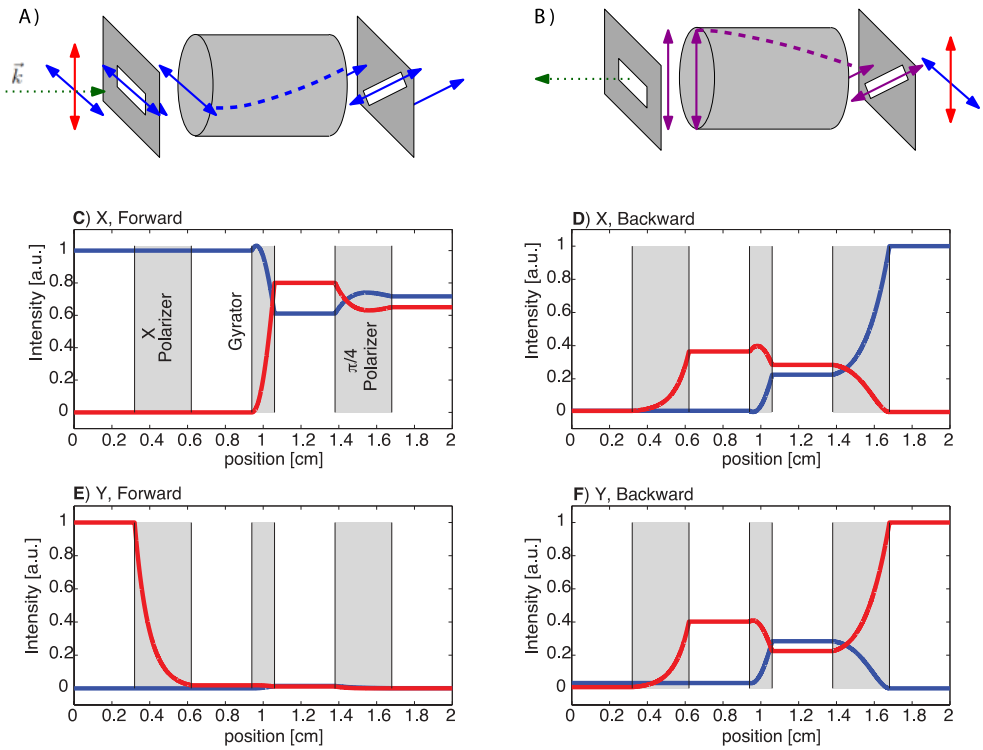

FIG. 1. (A), (B): Schematic diagram for an isolator (diode). Constructed of a gyrator (cylinder) between by two polarizers (rectangles, gaps indicate the polarization that is allowed to pass). Blue and red lines indicate the x and y polarizations, with purple ((B) only) being a superposition of both. Green lines denote the direction of signal propogation(the wavevector, $\vec{k}$). (A) Forward operation. Unpolarized signal enters, becomes polarized, gyrated, and then leaves. (B) Backward operation. Unpolarized signal enters, becomes polarized, gyrated, and then blocked. (C)-(F): Operation of a diode. Blue and red lines indicate polarized intensities. Grey rectangles indicate MA. (C) and (D) have the incoming signal x-polarized (allowed polarization), whereas (E) and (F) have the incoming signal y-polarized. (C) and (E) have the signal approaching from the front of the diode, while D) and (F) have the signal approaching from the back. Only in (C) is the signal transmitted. Figure from S. R. Sklan and J. C. Grossman, New J. Phys. **16**, 053029 (2014).[11]

1. Macroscopic Thermal Effects

At a macroscopic level, the coupling between channels can be controlled by thermal warping of a curved boundary which changes the effective area of the interface. When the thermal warping is mismatched, this can induce rectification, as reversing the direction of thermal gradient changes the thermal response in a way that exacerbates the asymmetry intrinsic in the curved boundary (see Ref. 16 as well as Ref. 14 and references therein). As is typical of thermal rectification, though, thermal warping induced rectification is often found simultaneously with thermal strain induced rectification.[17] While both of these interactions induce rectification, they do so in opposite directions. This competition between the different forms of rectification means that the direction of preferred transmission can be controlled by controlling the properties of the macroscopic interface.[18]

A far cleaner case than a homogeneous systems joined with boundary layers is possible by considering a single inhomogeneous material (which can be thought of as a composite of many homogeneous systems). In particular, if the thermal conductivity is not a separable function of position and temperature in the system, then this asymmetry in the conductivity can induce rectification.[19] This type of rectification follows simply from Fourier's $q = -\kappa(r,T(r))\nabla T$. For example, for a composite system of two layers with $q_R(T_H) > q_L(T_H)$ and $q_R(T_C) < q_L(T_C)$ where R, L are right and left side and H, C are hot and cold side, then heat flowing from right to left will be greater than the reverse. A simple model of this in terms of Fourier's Law for thermal conductivities following power law dependence on temperature is given in Ref. 20 where they find a rectification factor that linearly depends upon the size of the thermal gradient. This theoretical result agrees nicely with the

experimental data (for example Ref. 21) An important corollary of this result is that strong thermal rectification, from this mechanism, requires a large mismatch in temperatures.

2. Microscopic Thermal Effects

When moving from macroscopic to nanoscale systems, it becomes possible to control the system with far greater precision. However, trade-offs remain, as it is easy to create theoretical devices that outstrip the range of experimental techniques. This is further exacerbated by serious questions of the robustness of the theoretical predictions of thermal rectification. In the standard set-up, the system (often, a set of atoms with some pseudopotential or an anharmonic lattice of some asymmetric geometry) is placed in contact with two heat baths, one at each end. These heat baths are intended to approximate the outside environment, but care must be taken so that the choice of bath does not induce additional, artificial rectification effects. In Sun *et al.*[22] they consider a thermal rectifier attached to heat baths that are not impedance matched to the rectifier. Reflections of the thermal phonons from the boundary will pass through the rectifier (possibly multiple times), increasing the strength of the rectification. To address the question of intrinsic thermal rectification, they consider a pair of Fermi-Pasta-Ulam (FPU) lattices that individually obey the relation

$$\mathcal{H} = \sum \frac{p_i^2}{2m} + \frac{k(u_i - u_{i-1})^2}{2} + \frac{\alpha(u_i - u_{i-1})^3}{3} + \frac{\beta(u_i - u_{i-1})^4}{4} \tag{1}$$

and are joined by an interfacial link k_{int}. By using a new type of heat bath, which nearly eliminates reflections, they show that thermal rectification is an intrinsic property of their system. Romero-Bastida and Misael Arizmendi-Carvajal[23] meanwhile, consider the question of how their system's (an FPU β lattice (i.e. as eq. (1) but $\alpha = 0$) with linear mass gradient) coupling to the heat bath affects their results. In particular, because the ends of their lattice display localized edge modes, pumping heat solely into the ends of the lattice will be qualitatively different from thermostating an entire segment. They find, however, that it is precisely the case of only thermostating the ends of their system that results in the strongest rectification, with the effect diminishing as more of the lattice is thermostated. A further issue with thermostats is found by Lee *et al.*[24] They use molecular dynamics (MD) to consider a nanocone geometry, such as is achieved in an AFM tip, with each side of the cone coupled to a large thermostat. Because there is greater contact at the wider end of the cone than the narrower, heat flow is necessarily asymmetric for the forward and reverse configurations. This rectification vanishes, however, when the thermostat on the wider face shrinks to a comparable size as the narrower face's.

Despite these scruples, a great deal has been achieved in nanoscale thermal rectifiers. Structural effects, where the system tapers to a bottleneck, have proven particularly popular as they do not necessarily require inhomogeneous materials. Phonons propagating along the forward direction are funneled through, while only a small number can pass through the narrow opening in the reverse configuration (see Refs. 12–14 and 24 and references therein). In addition to this purely ballistic effect (which requires a sharp narrowing in the reverse direction and a gentle narrowing in the forward direction), though, the narrowing of the nanostructure induces phonon confinement. Wang *et al.*[25] consider a trapezoidal sheet of graphene and perform non-equilibrium MD (NEMD) simulations of the heat transport for various configurations. For sufficiently wide trapezoids, they find no thermal rectification. However, as the trapezoid narrows, phonon lateral confinement becomes prominent and induces thermal rectification. This confinement is found to have a number of effects. First, for narrow regions the phonon spectrum and vibrational density of states (vDOS) becomes dependent on width and temperature. This results in a mismatch between the phonon modes at each end of the trapezoid. Second, this dependence also implies that throughout the trapezoid the thermal conductivity is no longer separable. This is because

$$\kappa \propto \int d\omega v_g(\omega)\lambda(\omega)\hbar\omega D(\omega)\frac{\partial n(\omega,T)}{\partial T} \tag{2}$$

(where ω is frequency, v_g group velocity, λ mean free path, D vDOS, and n phonon distribution) has a position dependence for D (the previous effect) but also λ. Third, confinement induces localized

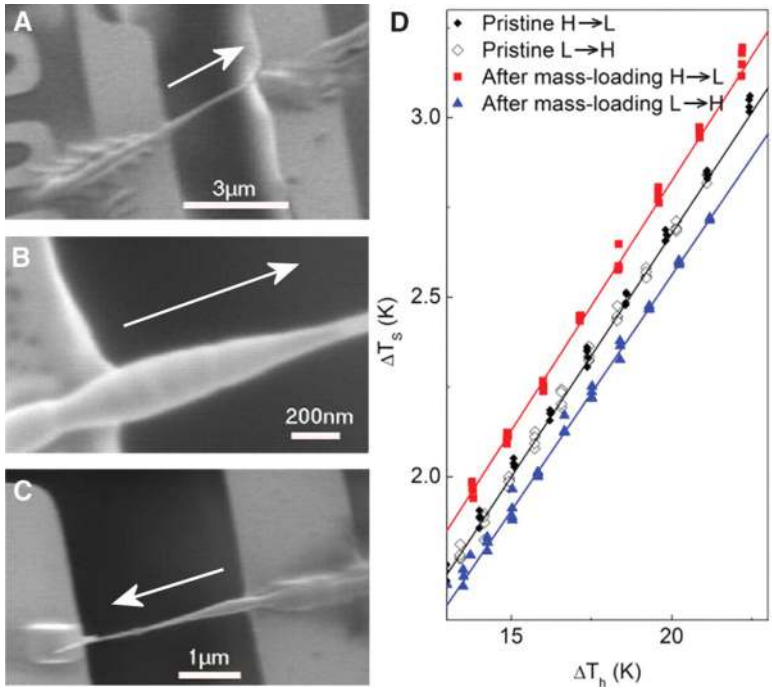

FIG. 2. (A)-(C): Scanning electron microscope images of boron nitride nanotubes after deposition of 7, 4, and 3% C_9H_16Pt respectively. (D)Temperature change at sensonr (ΔT_s) vs temperature change at heater (ΔT_h) for the BNNT before and after deposition. Figure reprinted with permission from C. W. Chang *et al*., Science **314**, 1121 (2006).[26] Copyright 2006 AAAS.

modes around the edges of the nanoribbon. This in turn effectively softens those phonon modes to a lower frequency, changing the transmission characteristics of the system. These three effects are not all independent in a confined system, but the precise relation between them remains indeterminate.

Perhaps the most fruitful asymmetric structure for thermal rectification is the linear mass grading. This is was the first system where nanoscale thermal rectification was experimentally observed. Chang *et al*.[26] observed rectification in carbon and boron nitride nanotubes. One end of the nanotube was coated with Trimethyl-cyclopentadienyl platinum to produce a cone. While rectification was clearly observed (see Fig. 2), the origin of this effect is still subject to debate.[27] It was originally argued that nonlinear effects in this system produced solitons that were responsible for the rectification.[26] Alaghamedi *et al*.[28] performed NEMD simulations of nonuniform mass carbon nanotubes. They found that anharmonicity and nonuniform mass were sufficient for rectification, but did not address soliton formation. Pereira,[29] on the other hand, addresses the problem from a purely analytic expression of heat transport for a graded material demonstrating nonseparable conductivity. Considering a model where the heat flux at a site is determined by the temperature difference at the adjacent sites ($T_j - T_{j+1}$) and a thermal resistance that's the average of the resistance at each site. In particular, when the thermal resistance at each site follows a power law with exponent a, he finds a rectification factor proportional to $T_1^a - T_N^a$. Note that this depends only on the temperature difference across the lattice, but that it's no longer simply a linear function of temperature difference, as was found in Ref. 20.

Since anharmonic, nonlinear effects are so central to thermal rectification, the role anharmonicity alone – without artificial structure – has also been considered. This work has generally been for pairs of 1D nonlinear chains, like the FPU lattice. Terraneo *et al*.[30] initiated this subject in 2002 with their study of a harmonic lattice with a Morse on-site potential

$$H = \sum \frac{p_n^2}{2m} + D_n\left(e^{-\alpha_n y_n} - 1\right)^2 + \frac{K(y_n - y_{n+1})^2}{2} \tag{3}$$

which was invented for modeling DNA. When D_n and α are inhomogeneous, specifically when the edges have different values from the center (as might occur for a different base pair), they find rectification. This concept was extended in Li *et al.*,[31] where they use a Frenkel-Kontorova (FK) lattice model

$$H = \sum \frac{p_n^2}{2m} + \frac{k(y_n - y_{n+1} - a_l)^2}{2} + \frac{V_0}{4\pi^2}\left(1 - \cos\frac{2\pi y_n}{a_s}\right) \tag{4}$$

which models (for example) a film strained due to lattice mismatch with its substrate (see also Ref. 13). (For the mismatched substrate, a_l is the equilibrium separation between sites and vanishes when y is the displacement from equilibrium rather than the position, a_s is the substrate periodicity which may be incommensurate with a_l, and V_0 is the effective substrate-lattice coupling strength.) By using two different FK lattices in series, they find strong overlap of the phonon bands in the forward configuration and little overlap in the reverse, leading to rectification. Hu *et al.*[32] also consider a pair of FK lattices with an effective coupling, but take the work of Li *et al.*[31] to new regimes. In particular, they examine parameter values that were previously neglected. Doing so, they observe a reversal of the direction of thermal rectification by changing the size of the thermal gradient. This can be seen as a competition between thermal effects and the coupling strength. At high temperature, the lattices are weakly coupled and rectification is dominated by temperature-dependent band alignment. At low temperature, the lattices are strongly coupled and rectification is dominated by band mixing across the interface. These two rectification effects (mode hybridization and band alignment) are in competition with each other, each of them drives rectification in an opposite direction. Examining a pair of not only asymmetric but also inequivalent lattices was begun by Lan *et al.*[33] where they demonstrate rectification in an FPU lattice coupled to an FK lattice. The presence of rectification in this variety of lattices and combinations suggests that the rectification effect is robust to the particular choice of model.

3. Phase Change Thermal Rectifiers

One concept that has gained attention subsequent to previous review papers is the idea of using phase transitions to induce rectification. This is an intuitive extension of the temperature dependent thermal conductivity scenario, where the change of phase produces a discontinuous change of conductivity and thereby breaks reciprocity. This does not necessarily require an inhomogeneous system, however. Komatsu and Ito[34] perform NEMD simulations of a box of homogeneous fluid in contact with a pair of asymmetric thermostats. One thermostat covers the entire side while the other is only a small region. Such a configuration is already likely to produce an artificial rectification effect, as in Ref. 24, but also displays an additional rectification effect. When the smaller thermostat is hotter, the liquid vaporizes in the vicinity of the thermostat, weakening its coupling. In contrast, when the larger thermostat is hotter vaporization is opposed by the pressure that such a packing would produce, so the system remains a (superheated) fluid. Kobayashi *et al.*[35] worked on a composite system of MVO (MnV_2O_4) (which has a phase transition between two solid phases at 57K) and LNCO ($La_{1.98}Nd_{0.02}CuO_4$). Unlike most previous work on interfacial rectifiers, they do not use equal length samples of MVO and LNCO, working instead with 3mm and 7mm segments, respectively. These lengths are selected such that $\kappa_{LNCO} = \sqrt{\kappa_{MVO,L}\kappa_{MVO,H}}$ where L, H refer to the low and high temperature phases of MVO. Based upon theoretical work by Peyrard[36] for temperature dependent conductivity (similar to Refs. 19 and 20) for nanoscale systems (specifically a Morse lattice), it is predicted that such a thermal conductivity would maximize the rectification coefficient to a value $R = |q(\Delta T)/q(-\Delta T)| = \sqrt{\kappa_{MVO,L}/\kappa_{MVO,H}} > 1$. They observe a comparatively large rectification coefficient ($R = 1.14$) for a comparatively small thermal gradient (2K). Garcia-Garcia and Alvarez-Quintana[37] consider a similar scenario to Ref. 35, extending the model to consider both conductivity dependent effects and interfacial effects due to acoustic mismatch. They use a Nitinol bar, which undergoes a solid-solid phase transition, as well as several other stable media (Cu, Fe, graphite) to determine the role of acoustic mismatch in rectification. When there is a mismatch between the modes at an interface, heat can still flow but is subject to an interfacial thermal resistance (Kapitza boundary resistance), which is known to also play a role in thermal

rectification.[13,38] They use a setup where the hot side is warmed by a resistive heater and the cold side is cooled by a Peltier element. When the Nitinol is heated above it's transition temperature ($\Delta T \approx 38K$) in the forward configuration and attached to the Peltier in the reverse, they find clear rectification for a range of temperatures. However, increasing the temperature at the heater in the reverse configuration increases the temperature throughout the system, eventually reaching a point ($\Delta T \approx -100K$) where the Nitinol undergoes a phase transition. This allows them to divide the $q - \Delta T$ curve into forward bias, reverse bias, and breakdown regimes, in analogy with an electrical diode.

4. Linear Acoustic Rectification

Although not a diode in the most rigorous sense (see s[12]), there has been considerable interest in what might be termed "bottleneck" effects. This is, in part, due to their relative ease of fabrication and role in injury reduction in ultrasonic treatments.[39] While in the thermal case, most of the interest was in tapering the structure, for acoustic systems the focus is often the inclusion of defects that induce a bottleneck. In particular, the use of triangular scatters[40] are a common approach, as the bottlenecking is fairly intuitive and the rectification can be directly observed in real-time as in Ref. 41 for surface acoustic waves (SAW) in porous silicon and Ref. 42 for sound in air with wooden rods. What's more, assuming a sufficiently low temperature (i.e. where ballistic acoustic transport dominates over diffusive thermal transport), thermal populations of phonons still exhibit this rectification[43] and so are effectively thermal rectifiers. As an analogous effect to triangular scatters, there is the use of asymmetric surface roughness in layered media. Both Sun *et al.* and Jia *et al.*[44,45] use layers of textured steel planes in water. In particular, from one side the planes are smooth, whereas from the other there are periodic rectangular bumps. The textured side allows the incident wave to be converted into modes that can propagate through the steel plate, whereas from the smooth side there is much weaker conversion. This is therefore related to mode-mismatch techniques. The texturing does not need to be attached to the layer (see Fig. 3(b)), as demonstrated in Sun and Zhang[46] for an array of spherical scatters in front of a series of smooth planes of brass in water. Zhu *et al.*[47] use an interface of two phononic crystals (PCs)[48] in a wire to create a Lamb wave rectifier. The PCs are constructed from tungsten blocks in a silicon matrix, with one PC an antisymmetric array (top-bottom-top) and one PC symmetric (superlattice of tungsten and silicon). An antisymmetric wave incident on the antisymmetric grating hybridizes with the symmetric mode, while the symmetric grating blocks the asymmetric mode and only passes the symmetric. Conversely, an asymmetric mode incident on the symmetric grating is blocked. By changing the stress

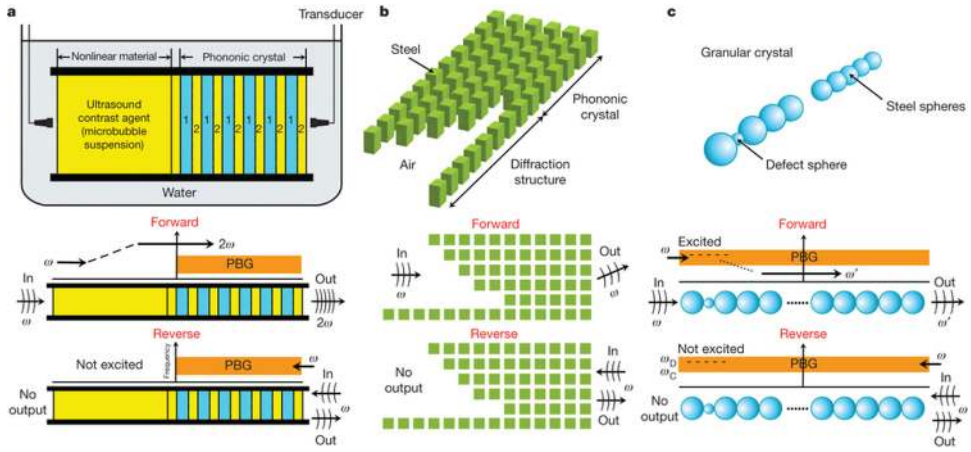

FIG. 3. Acoustic Diodes. (A) Diode constructed from a nonlinear medium and phononic crystal filter. As in Ref. 54. (B) Linear diode based upon asymmetric diffraction, as in Ref. 81. (C) Diode from nonlinear granular lattice, with defect serving as mode conversion and lattice serving as filter. As in Ref. 62. Figure reprinted by permission from M. Maldovan, Nature **503**, 209-217 (2013).[9] Copyright 2013 Macmillan Publishers Ltd: Nature.

loading on the silicon rod, this can be changed so that the roles of the symmetric and antisymmetric modes are swapped.

An alternative approach to scattering based rectification uses gradient materials. Li *et al*.[49] studies a gradient index PC where the PC is composed of circular scatterers of varying diameter. On one face, there is a narrow gradient along the direction of normal incidence and along the opposite face there is a broad gradient set at an angle. At the sides of the system are perfectly absorbing boundaries. Rectification here can be understood in terms of ray tracing. The angled gradient causes sound waves to curve. Along the forward direction (angled gradient first), this curvature is such that sound entering from the narrowest section comes out on opposite side of the crystal (the rest is absorbed at the boundaries). Along the reverse direction, the wave bends in the same direction, so the entire signal hits the absorbers. Chen *et al*. and Lu *et al*.[50,51] examine SAW and Lamb waves in PC slabs (composed of a grating with gradient depth). As in the textured slab cases, these studies worked by mode conversion – in particular the conversion of an antisymmetric to a symmetric wave via $A + S$ hybridization in the forward configuration and no hybridization in the reverse. Lu *et al*.[51] pair this geometry with an asymmetric double slit source, using the interference of the signals to enhance rectification.

The scattering of phononic crystals has other useful features for inducing rectification. Yuan *et al*.,[52] consider a PC within a bent waveguide. The PC is designed so that it has a partial band gap along the ΓX direction of the Brillouin zone but not the ΓM direction. As such, waves approaching the PC head-on are blocked by the partial band gap while waves approaching along the bent segment of the waveguide are incident upon the PC at an angle and can pass through. Another approach to this angle-dependent PC rectification was undertaken by Cicek *et al*.[53] for a pair of PCs (aluminum cylinders in air, more often called sonic crystals). The PCs are given cylinder radii, and lattice constants, resulting in very different Brillouin zones. They are also oriented differently at the interface, so that incident waves from each side will be at different angles and so different vectors in the Brillouin zone. For waves incident in the forward configuration, the first PC rescales the wave-vector but does not alter its direction. In crossing to the second PC the wave-vector is refracted, producing a transmitted signal at a new angle (as well as a second transmitted signal with k vector separated by a reciprocal lattice vector from the primary transmission peak). For waves in the reverse direction, though, they are incident on the second PC in the direction of a partial band gap, and so are blocked. This combination of filtering and mode conversion used in Refs. 47, 50, and 53 is linear, but is closely related to the nonlinear PC methods of the next subsection.

5. Nonlinear Acoustic Rectification

The scattering focused work on hybridization relied upon purely linear, reciprocal effects that mixed modes of the same energy but different symmetry. An obvious extension of this work, which at least in principle breaks reciprocity,[12] is nonlinear mode conversion. Liang *et al*.[54] is emblematic of this approach. Their system is a PC superlattice (layers of water and glass) connected to a nonlinear fluid medium (see Fig. 3(a)). The PC has a gap at the incident frequency. The nonlinear medium, however, generates a second harmonic wave at twice this frequency. Thus, waves incident on the PC are damped, whereas waves incident on the nonlinear medium become a combination of fundamental and second harmonic modes, the latter of which can pass through the PC. The frequency dependence of this system was further resolved in Ref. 55, where they examine the rectificatied transmission for the different band gaps of the PC. This approach was experimentally realized in Liang *et al*.[56] (and later numerically optimized in Ref. 57). The PC was again a water-glass superlattice, and the nonlinear medium was an ultrasound contrast agent (UCA) microbubble suspension. The bubbles can expand or contract with the acoustic excitation (see Ref. 57), creating the nonlinear response required for second harmonic generation. Ma *et al*.[58] extend this work from a superlattice to a one or two dimensional lattice of harmonic oscillators. They numerically optimize the motif of masses and springs to block the fundamental mode but pass an integer multiple of the fundamental mode, finding that a triatomic lattice is preferred in 1D (but is comparable to a diatomic lattice in 2D. They then attach a Duffing oscillator (a nonlinear oscillator) to generate a third harmonic signal, resulting in a band of strong rectification.

Inspired by Ref. 54, Lepri and Casati[59] take a slightly different approach. They still use a composite of two different materials, but the filtering and nonlinearity are shared by both materials. Specifically, they consider a pair of lattices that each obeys the discrete nonlinear Schrödinger (DNLS) equation

$$\omega\psi_n = V_n\psi_n - \psi_{n-1} - \psi_{n+1} + \alpha_n|\psi_n|^2\psi_n \tag{5}$$

but have different values of V and α. One advantage of the DNLS over other lattice models is that it can be solved analytically for traveling waves, a fact that allows them to explicitly calculate the transmission for each direction of propagation. They demonstrate that even if each DNLS layer is one site thick (i.e. a dimer defect in a linear, harmonic lattice), there are values of frequency and incident intensity that produce rectification. In particular, for a given frequency and direction of incidence, the transmission coefficient bifurcates as a function of intensity, jumping from low intensity transmission to high(er) intensity transmission (or vice versa). The location of these bifurcations is asymmetric for the different directions of incidence, however, so there exist windows where the transmitted intensities are sharply different (see Fig. 4). A direct simulation of the system for Gaussian wavepackets confirms this property, with strong reflection of the blocked beam and weak reflection of the transmitted beam. Assunção *et al.*[60] extend Lepri and Casati work on DNLS rectifiers to the case of saturable rectification ($\alpha_n|\psi_n|^2 \to \alpha_n|\psi_n|^2/(1+\beta_n|\psi_n|^2)$), a similar trade-off to the FPU vs. FK lattice rectifiers in the thermal rectification section. They find that while excess saturation can eliminate some of the rectification windows, it will broaden the remaining ones. Li and Ren[61] consider geometric effects with DNLS. They analyze triangular segments of a DNLS lattice with homogeneous coefficients, finding rectification even when the contact width is the same for both faces. By tailoring their geometry and layering rectifiers in series, they are able to control the direction and magnitude of this rectification, making their approach more readily tunable than the inhomogeneous DNLS model.

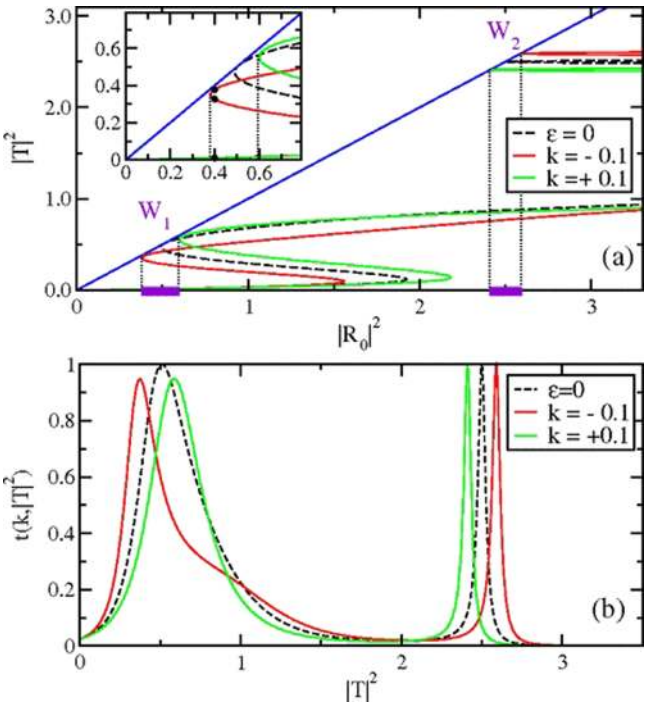

FIG. 4. Acoustic rectification via bifurcation. (A) Transmitted intensity $|T|^2$ as a function of incident amplitude $|R_0|^2$. Black lines are the linear case, red and green are the two directions of incidence for the nonlinear case. Bifurcation windows are indicated in purple. (b) Transmission coefficient vs. transmitted intensity. Figure reprinted with permission from S. Lepri and G. Casati, Phys. Rev. Lett., **106**, 164101 (2011).[59]

A third approach to nonlinear acoustic rectification was developed by Boechler *et al*.[62] They use a 1D lattice of macroscopic metal spheres with Hertzian contact. By changing the initial compression force on the spheres, the spheres' deformation from equilibrium can be changed, thereby modulating the nonlinearity of the Hertzian contact. Furthermore, this lattice will exhibit a band gap above a critical frequency. Inserting a defect (a sphere with a smaller diameter) near one edge of the lattice will result in a localized defect mode with a frequency in the band gap (see Fig. 3(c)). Upon the excitation of this mode, nonlinear effects within the rest of the lattice will down-convert the signal into propagating modes within the acoustic pass band. Conversely, driving the lattice at the defect frequency from the end far from the defect will not excite any appreciable amplitude vibration. As such, the nonlinear down-conversion will not occur and the signal will not propagate. As with the other nonlinear rectifiers, this system exhibits an amplitude dependent bifurcation in the forward configuration. Low amplitude driving will fail to produce sufficient amplitude for down-conversion, so no signal can propagate. Merkel *et al*.[63] examine a 3D granular phononic crystal. Their system is not only compressed vertically, but they also analyze the role of gravity in their treatment. Since each layer will experience a force due to the weight of the layers above it, this creates an inhomogeneous compression. They experimentally and numerically observe that this inhomogeneity results in asymmetric transmission of longitudinal modes moving with or against the direction of gravity. This effect can be partially tuned by controlling the initial compression.

Finally, Lepri and Pikovsky[64] use nonlinearity to create a "chaotic diode". Their system is a pair of dissimilar nonlinear oscillators (quartic potential, as in the FPU β lattice) connected to each other by a harmonic string. Waves traveling along the string will interact with the oscillators. Because the string is perfectly nondispersive, signals from one oscillator will reach the other only after a delay, meaning that the pair of oscillators interact with each other through effectively a delay different equation. For weak coupling they analytically find only weak frequency conversion to higher frequencies and amplitude-dependent bifurcations in the transmission, similar to the DNLS based rectifiers. Furthermore, when the delay time decreases, the system begins to resemble a photonic Fabry-Perot resonator coupled with two off-channel defects. Numerically, they find solutions that approach a fixed point or limit cycle, with broken reciprocity demonstrated by the conversion of a periodic driving signal to a constant output (as in the original sense of rectification). When there is no separation of time-scales (i.e. not weak coupling or negligible delay), chaotic solutions are possible and numerically integration is necessary. In particular, they find scenarios where the transmission of a signal in one direction is periodic while the transmission in the other is chaotic.

B. $\mathcal{T}$ Symmetry

Breaking time reversal symmetry is much harder than breaking parity, there are only a small number of options available. The classic method for breaking time-reversal symmetry is to include a magnetic field. This is done in the photonic equivalent of a diode, an optical isolator. An isolator is composed of three elements in series: a linear polarizer, a 45° Faraday rotator, and a second polarizer oriented 45° from the first (see Fig. 1). The Faraday rotator is a material that, when subject to a magnetic field, effectively rotates the angle of polarization. Thus an unpolarized signal approaching from the front becomes linearly (let's say vertically, for concreteness) polarized, rotates 45° and passes through the second polarizer without dissipation. An unpolarized signal approaching from the back, however, becomes polarized along 45° and rotates in the same sense as before when it passes through the Faraday rotator (this is the effect of the broken time-reversal symmetry). Hence, the signal is horizontally oriented when it reaches the first polarizer, and is strongly suppressed. In Sklan and Grossman[11] they translate this concept to a phononic system. Since there is no direct coupling of the magnetic field to phonons, as there is for the optical case, they use magnetic materials with an effective magnon-phonon coupling (such as magnetostriction). The magnon-phonon interaction is strongest when the two waves are in resonance, and this resonant frequency can be tuned by applying a magnetic field (which shifts the magnon spectrum). They use the dependence of the magnon-phonon interaction on the direction of the (local) magnetic field to produce both the polarizers and the Faraday rotator. In particular, when the magnetic field is oriented parallel to the phonon wavevector, there is an acoustic Faraday effect that rotates the angle of phonon polarization

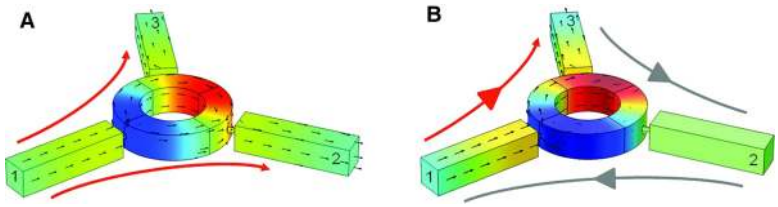

FIG. 5. Rotational rectification. (A) When no rotation is applied to the ring, signals propagate equally through each branch. (B) When rotation is applied, the broken symmetry suppresses the signal along one branch. Figure reprinted with permission from Fleury *et al*., Science **343**, 516 (2014).[65] Copyright 2014 AAAS.

(i.e. circular birefringence, albeit with a different functional dependence). Moreover, when the magnetic field is oriented perpendicular to the phonon wavevector, there is an acoustic Cotton-Mouton effect that induces linear dichroism (linear polarization dependent damping). Unusually for polarizers, this damping is polarization dependent, with only the mode polarized parallel to the magnetic field experiencing any loss from the Cotton-Mouton effect. For their geometry, only transverse polarized phonons can be affected by this isolator design, there is no effect on longitudinal phonons (which is expected given that optical isolators only effect transverse photon modes).

Fleury *et al*.[65] take inspiration from the electronic Zeeman effect to break reciprocity. However, instead of using a magnetic field they use a rotating frame, as the Coriolis force is analogous to a magnetic field. They consider acoustic waves in air, rotated by a fan in a circular chamber. The chamber is linked up to three equally spaced channels. When a wave enters one channel, it will travel along both the clockwise and counterclockwise paths to reach the exits. The phase difference between these two waves (and therefore the transmission) at each exit can be tuned by controlling the fan speed. Waves moving with or against the direction of rotation effectively experience Doppler shifts to frequency $\omega \pm \omega_{Cor}$. They calculate (see Fig. 5) and experimentally observe that for the right value of the rotation speed, there is no transmission through one exit (say, channel 1 to 3) and enhanced transmission through the other (say, channel 1 to channel 2). On the other hand, a signal entering from this port would exit from the third one and not the original (i.e. 2 to 3).

C. $\mathcal{PT}$ Symmetry

Systems that break both time reversal and parity symmetry (but preserve the symmetry of $\mathcal{PT}$) have recently gained prominance for their potential to break reciprocity. These systems are often active, incorporating gain and loss media (see Fig. 6). In terms of lattice models or quantum systems, this means that the system is non-Hermitian but its potential obeys the relation $V(x) = V^*(-x)$. D'Ambroise *et al*.[66] examine the DNLS system, where a small number of sites (2-4 or N) have acquired a complex potential V. Unlike previous work with DNLS lattices, the Re(V)

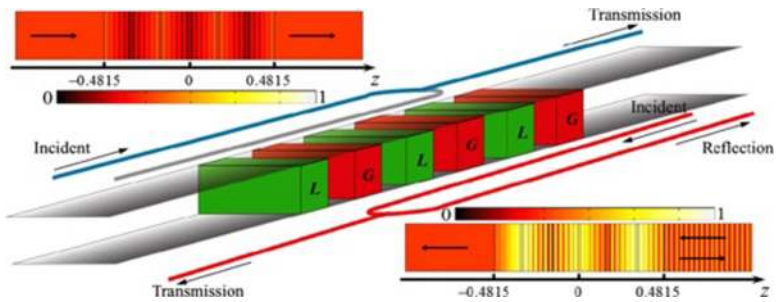

FIG. 6. Schematic of a $\mathcal{PT}$-symmetric medium. Regions of loss and gain are red and green respectively. Blue and red lines denote different directions of incidence. Insets: The amplitude for the left (left inset) and right (right inset) incidences at the point of unidirectional transparency. Figure from X. Zhu, H. Ramezani, C. Shi, J. Zhu, and X. Zhang, Phys. Rev. X **4**, 031042 (2014).[67]

and α are symmetric, the asymmetry comes from Im(V) being antisymmetric. That is, depending on which side a wave approaches from, it will hit a gain or loss (segment first. While a great deal of energy often became localized to the PT-symmetric oligomer, this was mainly due to the gain medium so there was still appreciable transmission and rectification. In particular, it will be transmitted if it hits the gain medium first, and blocked if it hits the loss medium first. A similar approach was taken in Zhu *et al.*,[67] except they considered acoustic waves with $\kappa(r) = \kappa^*(-r)$ and $\rho(r) = \rho(-r)$. Analytic calculations indicate that the system undergoes a bifurcation as a function of frequency, with the reflected amplitude of the wave incident along initial loss direction vanishing at this critical frequency (see Fig. 6). In addition to rectification, both Refs. 66 and 67 find that gain means the transmitted signal can be amplified to above its initial intensity.

Zanjani *et al.*[68] study a plate acoustic waveguide containing a modulation domain. Within the modulation domain, the acoustic properties (stiffness, density) are spatially and temporally modulated by a traveling wave. An acoustic wave traveling in the direction of the modulation wave and of the appropriate frequency will by converted to a new mode, while a wave traveling the opposite direction will not. Once the direction of propagation has been isolated in this way, filtering allows the selective passage of only one direction of phonons.

Finally, Popa and Cummer[69] consider a metamaterial composed of a piezoelectric membrane sandwiched between two asymmetric Helmholtz resonator cavities. The asymmetry of the cavities means that they transmit different frequency modes. The piezo is also attached to a nonlinear circuit that takes the measured signal from the desired direction and converts it into the signal needed to pass through the other cavity. Signals from the opposite direction, however, are filtered out by the resonator and the electronics.

II. TRANSISTORS AND SWITCHES

In electronic computing, a transistor is a device that acts like a switch and an amplifier. It has three terminals, a source, a gate, and a drain. A signal at the gate can block the flow of current from source to drain. Amplification arises because small changes in the signal at the gate can result in large changes in the output signal at the drain. In a phononic context, the central problem is one of control, of finding a way to make the state of one phonon current dependent upon the state of another. The most fundamental approach is to a directly controlled transistor, where (say) anharmonic interactions between phonons are the source of the transistor effect. But there are also indirect control schemes that are possible. In many scenarios, the phonon current can be readily controlled by some non-acoustic signal. Such devices can serve as switches. But if measurement of some phonon current's state is sufficient to activate this switch, then that phonon current indirectly controls the other. Therefore, these switches can work as indirectly controlled transistors.

A. Direct Control Transistors

In Li *et al.*[70] they studied three FK lattices linked in a T-shaped junction. For a range of temperatures, they demonstrate that the junction exhibits negative differential thermal resistance (NDTR) as a function of gate temperature (source and drain temperatures held fixed). NDTR implies that $-\partial J/\partial T < 0 < \kappa$, i.e. that increasing thermal bias decreases thermal current. So, by changing the temperature at the gate, the system can go from a state of low thermal current between source and drain ("off" state) to large current ("on" state). Furthermore, this effect is independent of thermal currents between the gate and drain, for they find three points ("off, semi-off, and on" states) where this current vanishes. Crucially, the operation of the transistor at these points is stable. This bistability is inherently nonlinear and a direct corrolary of NDTR. It also differentiates the operation of the thermal transistor from such trivial cases as $T_{Gate} \ll T_{Source}, T_{Drain}$ where thermodynamics implies that a net current only flows from the gate. They also find that, when the coupling of the gate segment to the drain is adjusted, the system goes from this switching behavior to an amplifier. For their setup, amplification also requires NDTR. In particular, a falling thermal resistance between (say) gate and drain, combined with a rising resistance between gate and source, allows the drain

to capture an increasing portion of heat flux with changing gate temperature. In Lo *et al.*[71] they increase the efficiency of this transistor model by using combinations of FK and FPU lattices and controlling the couplings between them. Another approach to thermal transistors was developed by Komatsu and Ito.[72] Unlike in the standard transistor model, where the gate lies between the source and drain, they place the source in the center, between the gate and drain. They fill the region between each terminal with molecules and use NEMD to model the heat transport as a function of gate temperature. When $T_G = T_D < T_S$ the molecules have condensed into a liquid along the drain and gate contacts, while they remain a gas near the source. This asymmetry suppresses the flow of current from source to drain. As the gate temperature increases and approaches the source temperature, the liquid phase now extends through the source-drain segment and allows for current flow (becoming equal to the current emitted by the source when $T_G = T_S$).

Alagoz and Alagoz[73] study acoustic transistors using a phononic crystal. Using a square PC with sources on adjacent sides (source and gate), they create a pair of sound waves that scatter off the PC and interfere with each other. At the drain side they numerically find and experimentally confirm two regions of constructive interference at the sides of the PC's face and destructive interference in the center. Using just this region of destructive interference for the drain, the addition or removal of a signal at the gate has a strong effect on the transmission at the drain.

The problem of an anharmonic phonon transistor was studied by Hatanaka *et al.*,[74] where they study phonon propagation in a 1D electromechanical resonant array. Their system was composed of a series of mechanically coupled piezoelectric membranes. This array can support a localized oscillation in the central membrane as well as a pair of extended modes that can travel the length of the array. When the highest frequency mode (an extended mode) is driven at one side, it can be suppressed at the opposite side by the excitation of the localized mode (or other extended mode) at the central membrane. This effect is analogous to electromagnetically induced transparency. Treating the higher frequency mode as the source and the other modes as the gate allows them to construct a transistor from this array. This work was extended for greater control of phonon propagation in Hatanaka *et al.*[75] They again constructed phonon waveguides by linking an array of membranes, albeit a longer array than Ref. 74 used. The bandstructure, phonon velocity, and transmission spectrum were all tunable by changing the dimensions of the membranes. Furthermore, they incorporated the techniques of Ref. 74 and inserted a defect in the lattice to serve as a cavity, thereby turning the waveguide into a switch via NEM-induced transparency (see Fig. 7).

Vanhille and Campos-Pozuelo[76] developed their model of an acoustic transistor from previous work on acoustic rectifiers using bubbles in ultrasound contrasting agent (see Ref. 56). They use a nonlinear medium with a bandgap at the original the original frequency. In addition, they use a low-frequency wave transverse to the original signal. This second signal creates a standing wave in the UCA, creating a pressure antinode near its source. The bubbles in the UCA are drawn to this region of low pressure, turning the UCA into a linear medium and thereby allowing transmission (see Fig. 8). Liang *et al.*[77] extended this approach to a more conventional design (specifically, a parametric amplifier). They also use the convert-and-filter design and bubbly UCA, but use low-pass instead of high-pass filters. They also use a pair of nonlinear media and filters, giving them a stronger amplification. In their design, a weak low frequency signal (ω_s) mixes with a strong high frequency pump signal (ω_p) to generate anharmonic signals at $\omega_p \pm \omega_s$. The first filter blocks any signal above $\omega_p + \omega_s$, which then interacts in the next nonlinear segment to amplify the ω_s signal. The final filter blocks signals above ω_s, including $\omega_p - \omega_s$. On the other hand, Li *et al.*[78] sought to translate the granular rectifier[62] design into a transistor. They use a chain of compressed metal spheres with Hertzian contact, driven at a frequency f_o above the cutoff of the acoustic band-structure. Normally, such a signal is blocked. But when a control signal (at f_c) at a frequency below the cutoff is added, the two will interact anharmonically to generate frequencies of the form $nf_0 \pm mf_c$ (n, m integers). Some of these signals (e.g. $f_o - f_c$) will be below the cutoff and can again propagate. This propagating signal will also interact with the control signal, generating signals with frequencies in the bandgap. This includes the original signal at frequency f_o, so the control signal allows the original signal to propagate through the bandgap. An approach within this framework, but in an unrelated system, was presented by Li *et al.*[79] They use a 1D array of helically stacked cylinders to create a helicoidal phononic crystal. The inter-cylinder angle is perturbed by

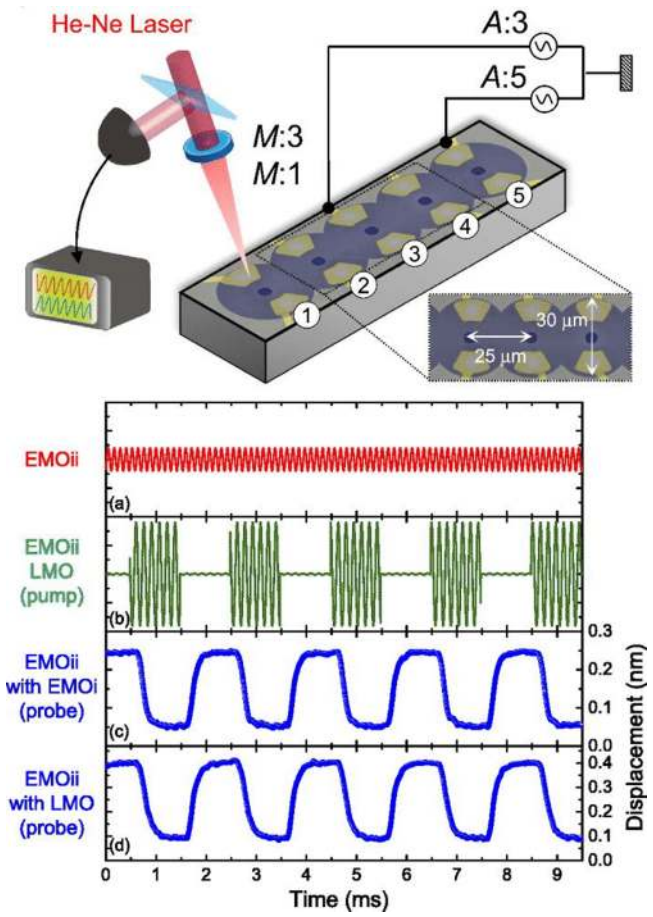

FIG. 7. Operation of a NEM transistor. (top) model of NEM array. (bottom) red (A) is source signal, green (B) is gate, blue (C)-(D) is drain. (C) and (D) use different pump modes for the gate. Reprinted with permission from Appl. Phys. Lett. **102**, 213102 (2013).[74] Copyright 2013 AIP Publishing LLC.

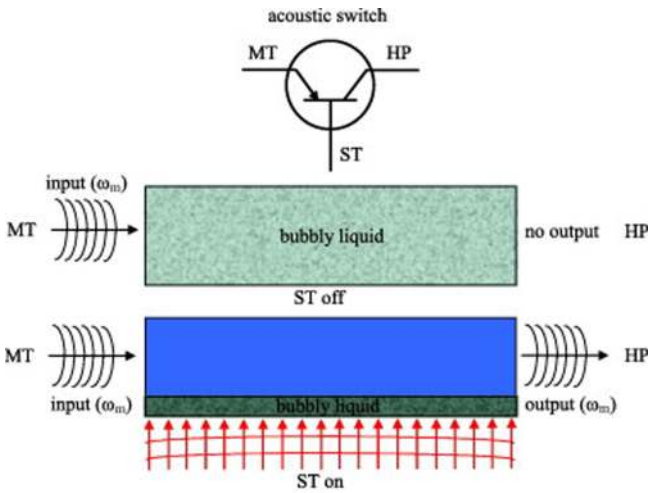

FIG. 8. Operation of an acoustic transistor. The bubbly liquid acts like an insulator at the original frequency, but the bubbles can be pushed aside by a second signal, thereby allowing the first to pass unimpeded. Figure reprinted with permission from C. Vanhille and C. Campos-Pozuelo, Ultrason. Sonochem. **21**, 50 (2014).[76] Copyright 2014 Elsevier.

torsional waves, inducing a nonlinear response. This can be exploited as in Ref. 78 by exciting a mode above the bandgap and letting it interact with a pump signal below the cutoff frequency, thus creating another implementation of this transistor design. While Refs. 77–79 use filters and nonlinearity, there are noticeable differences in their approaches. The first used a low frequency signal and filtered out their pump, while the latter two used a high frequency signal and restored it via a pump.

B. Switches and Indirect Control Transistors

V. F. Nesterenko *et al.*[80] initiated the granular material approach to phononics with their study of anomalous reflection in an array of granular crystals. They used a heterogeneous array, beginning with a ferromagnetic particle, then an array of 20 steel spheres, then an array of 21 polytetrafluoroethylene (PTFE) spheres. Waves were excited by striking the topmost sphere (i.e. the magnet). Normally, the waves would travel without appreciable reflection. But when the magnet was compressed by placing it between a pair of strong magnets, the resultant compression yields an impedance mismatch that produces strong reflections throughout the lattice and impedes the flow of energy. As such, the application or withholding of the magnets serves as a switch. Li *et al.*[81] combine the PC[54] and texturing[44] approaches to rectification to create an asymmetric PC (see Fig. 3(b)). Their PC (a series of rectangular rods) has one periodicity on one side ($a \times a$), and another on the opposite ($a \times 6a$) with intermediate layers being gradations between these limits. They find clear rectification when the rectangular rods' faces are aligned with the simple cubic lattice vectors, but when the rods are rotated 45° (so that the corners are aligned with simple cubic lattice vectors) the rectification vanishes. Along the direction of suppressed signal intensity, switching orientations effectively switches the transmission. Gunawardana *et al.*[82] takes a different approach to mechanical switching to produce a thermal switch. They consider an initially symmetric graphene nanoribbon. By applying an asymmetric strain, they break the symmetry of the system and create thermal rectification. This rectification can be tuned by changing the magnitude of the force applied.

Menezes *et al.*[83] moved away from these mechanical, anharmonic based designs and created an electronically controlled phonon transistor. They consider an infinite lattice constructed of polar molecules. At each end, the lattice is attached to a thermal bath, where the temperatures of both baths and the environment are sufficiently low that phonon transport is primarily ballistic. This lattice can support four modes, the three translational modes plus one torsional mode. When no electric field is applied, all of these modes are acoustic. But an electric field perpendicular to the lattice breaks the degeneracy of the torsional mode's rotation and shifts it into an optical mode. This shift results in a large change in the thermal conductivity, reducing it up to 25%. Jeong *et al.*[84] also consider electric field based control, reporting the first experimental observation of purely phononic switching (Zhu *et al.*,[85] report an earlier experimental observation of temperature controlled switching of a thermal rectifier, but their control was due to a transition between metallic and insulating phases and was therefore electronic, not phononic). They use a series of multiple quantum wells sandwiched between to piezoelectrics. These wells are built in pillars upon the substrate and electrical contacts are placed asymmetrically both on top of and between the pillars. In doing so, the application of a voltage difference between these electrodes will produce both a perpendicular electric field to counteract the piezoelectric field and also a lateral electric field. This lateral electric field will distort the symmetry of the lattice, breaking the isotropic structure into an anisotropic one. In doing so, the previously forbidden transverse acoustic mode is allowed to propagate. The frequency, amplitude, and lifetime all show signs of being tunable through the strength of electric potential.

Ben-Abdallah and Biehs[86] considered a thermal transistor incorporating near-field thermal radiation of photons. They separate the source and drain elements by a vacuum and place within the vacuum a thin layer of another material (in their case VO_2) to act as a gate. The gate material is selected so that it has a phase transition at a temperature between the source and drain's temperatures. This phase transition will change the transmission of particular photon modes, blocking them in one phase and allowing them in another. While their transistor is purely a photonic effect (albeit with thermal photon populations), they find that their transistor is particularly effective for photon

frequencies around the surface photon polariton resonance (hybridization of photons and phonons). At these frequencies, transmission is highly efficient in the pass state but vanishes in the blocked state. In principle, this would allow for an effective phonon transistor by using the surface phonon polariton modes to convertphonons to and from photons. Sklan and Grossman[87] took a somewhat more direct approach to the problem of switching by means of an optical control. They used a lattice composed of photoswitchable materials (i.e. photoisomers, ionic Raman active materials), modeling it as a bistable 1D harmonic lattice. Changing the intensity of light on the lattice increased the relative concentration of the photoactive state to the ground state, thereby shifting the bandstructure. This in turn shifted the location of the bandgap, allowing previously blocked frequencies to traverse the lattice.

Finally, in Sklan and Grossman[11] they present a fundamentally different approach to transistors. Throughout the previous work it has been implicitly assumed that information in the system (i.e. logical zero or one) has been encoded as either a temperature value (high or low) or phonon current strength (strong or weak). These encodings are perfectly reasonable, but they are based upon analogies with electronic computing, where information was encoded in high or low voltage and strong or weak electrical current. If inspiration comes from not electronic, but optical computing, the the method of information encoding changes. As a result, they encode information in the polarization (horizontal or vertical) of transverse phonons. Therefore, logic operations no longer need to block or pass a phonon current, but instead rotate its polarization between orthogonal values. Using a magneto-acoustic Faraday isolator (see section on $\mathcal{T}$ symmetry breaking diodes), this rotation is straightforward. They further extend this switching design to a full transistor be developing a circuit which converts the strength of a polarized phonon current to a constant magnetic field.

III. MEMORY

Memory is essentially a question of storage, of trying to maintain a phononic signal (e.g. temperature, amplitude, polarization) for as long as possible. All modes of decay limit the efficiency of memory, but the maintenance of a long-lived mode is not the only concern. It must also be possible to read and write the signal, meaning that some form of active control of the state (as in the section on switches and transistors) must be considered. Thus, the coupling of phonons to static and dynamic loss modes must be considered, as well as the balancing of the ease of writing against the need for stability.

Interestingly, phononic devices have a history as a memory system. Some of the earliest random access memory (RAM) was constructed out of acoustic delay lines, typically tubes filled with fluid where an acoustic signal could propagate until it was needed. These tubes were initially filled with mercury, although other designs (e.g. purely piezoelectric implementations) were considered. Turing, for example, famously suggested that gin would be a convenient medium.[88]

A. Thermal Memory

From the phononic perspective, work on thermal memory is still purely theoretical. Wang and Li[89] extended their previous work on thermal transistors[70] (built by FK lattices). For the on (off) state, there exists a point where the gate temperature pushes the drain temperature to a high (low) temperature but no current is drawn from the gate to the source or drain. At these points the gate segment can be safely decoupled without perturbing the drain temperature (see Fig. 9). However, without the stabilizing influence of the gate, other perturbations can shift the temperature from these values (but not far, the system exhibits stochastic stability). An attempt to realize this effect experimentally was given by Xie *et al.*,[90] but it relied upon a transition in electronic heat transport due to an insulator-metal transition and so is not a purely phononic device. Their approach bears much in common with recent work on phase change thermal energy storage (see Refs. 91 and 92 for an extensive review) and nanostructured thermal storage (recently reviewed in Refs. 92 and 93). While these works approached the problem from purely an energy management perspective, they still deal with the fundamental problems that are shared by phononic memory devices.

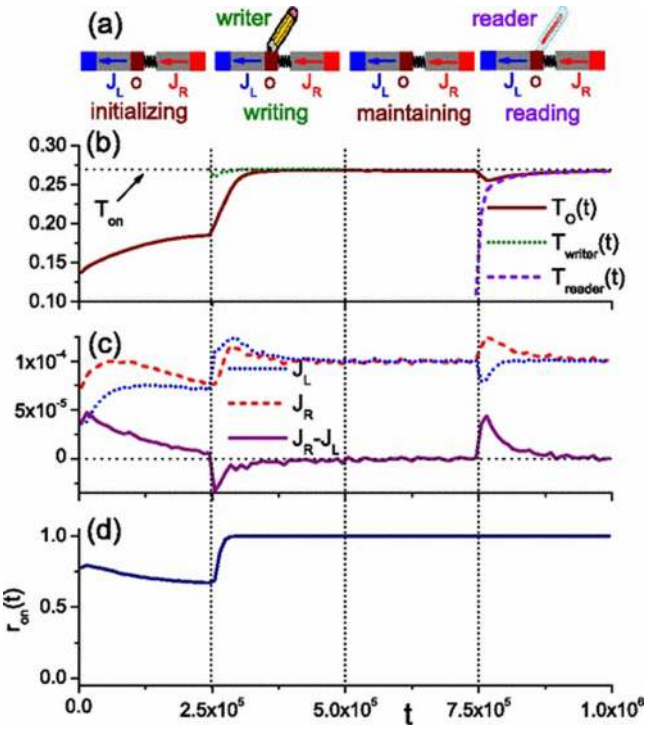

FIG. 9. Thermal Memory. (A) Schematic diagram of a write-read process on FK lattices. (B) Temperature profiles at the memory element (dark red), write head (green), and read head (purple). (C) Thermal current from the memory element going to the left (blue), right (red), and their difference (dark red). (D) Reliability over ensemble average of memory elements. Reprinted with permission from L. Wang and B. Li, Phys. Rev. Lett. **101**, 267203 (2008).[89] Copyright 2008 American Physical Society.

B. Phonon Storage of Non-Phononic Signals

Surprisingly, while much of phononic information processing has developed in isolation, the development of phononic storage systems has almost been the reverse. The generality of phononic interactions and (comparatively) long lifetimes has brought the attention of a number of unrelated fields to the problem of phononic storage. Many of these developments are focused upon the transduction of a signal to the vibrational mode of a nanoelectromechanical (NEM) oscillator. Much of the early work was based upon the static deformation of NEM via an electric field, as in Rueckes *et al.*[94] on carbon nanotube (CNT) arrays, but later work extended this to frequency-dependent phonon modes. Cleland and Geller,[95] used a piezoelectric membrane to store and transform signals between two Josephson junctions. Rabl *et al.*[96] take a similar approach to the coupling of spins using magnetized NEMs. The majority of the work in this field, however, has been undertaken by researchers in classical electronics and optomechanics.

Badzey *et al.*[97] extended the CNT oscillator approach to a frequency dependent case. They experimentally confirm that, when the CNT is driven by an AC current it behaves like a Duffing oscillator

$$\ddot{x} + 2\gamma\dot{x} + \omega_0^2 x \pm k_3 x^3 = F\cos\omega t. \tag{6}$$

A characteristic feature of the Duffing oscillator is its bistability, it exhibits hysteresis and jumps between two states as a function of amplitude and frequency. This jumping behavior means that a small, low frequency modulating signal can be used to switch the oscillator between its high and low amplitude states, which are maintained by a constant high frequency driving force. A similar bistable memory due to mechanical nonlinearity was found by Venstra *et al.*[98] for microcantilevers. Khovanova and Windelen[99] used the Pontryagin control approach to minimize the energy pulse needed to switch the NEM between states. Mahboob and Yamaguchi[100] used a suspended

silicon nanoribbon between two 2D electron systems to construct the mechanical equivalent of a "parametron," a bistable harmonic oscillator proposed as a logic device in the early stages of computer development. The frequency of the mechanical resonance was found to be tunable through a DC piezoelectric coupling. Because of the anharmonicity of the oscillator, the NEM oscillator exhibited resonance when driven at the resonant frequency and a parametric resonance of a modulated signal at twice the resonant frequency. When the oscillator is driven, it shows effectively no displacement below the resonant frequency (monostable), large net displacement (positive or negative buckling, or 0 and π phases, bistable) around the resonant frequency, and tristable (0 or π as well as no displacement) at frequencies above the resonant. The 0 and π phases are bistable and show hysteresis effects that allow for reading, writing, and storage of information. They demonstrate this by using an oscillator in the monostable regime, biasing it along one direction with a weak trigger pulse at the resonant frequency, and switching to the desire state (0 or 1) by applying a larger amplitude parametric actuator pulse at twice the resonance. When the trigger pulse ends, the system remains in its stable state, but when the parametric pulse ends it returns to the no displacement state. They extended this work in Mahboob *et al.*,[101] where they identify multiple parametric resonances for their system. Each of these frequencies can be addressed through the previous algorithm to store a bit of information as the displaced oscillations produced by these frequencies. Moreover, the information can be shifted between frequencies by means of anharmonic interactions between the parametric pulses.

In optomechanics, phononic storage was first considered by Zhu *et al.*[102] They considered the conversion of an optical pulse into an acoustic excitation by means of stimulated Brillouin scattering, a nonlinear electrostriction process induced by an interaction with a second optical signal. Specifically, the data is transmitted at a frequency above the read/write signal's by the frequency of excited phonon's frequency. Using wave-packets composed of many frequencies allows a wide spectrum of information to be stored, although it misses the highest frequency components (see Fig. 10). They experimentally demonstrate the storage of multiple signals as phonons within an optical fiber. But because the phonons themselves decay exponentially, the storage time for this technique was on the order of the phonon lifetime (i.e. nanoseconds for their system). An alternative approach was developed in Safavi-Naeini and Painter[103] and Change *et al.*[104] They used an optomechanical crystal (also called a phoxonic crystal), where defects simultaneously localized photons and phonons. Optical modes propagating through a waveguide became coupled to the optomechanical crystal, where they could then be reversibly converted into phonons via radiation pressure (see Fig. 11). Fiore *et al.*[105] translated this approach to a single optomechanical resonator, where the phonon lifetimes are significantly longer than in Ref. 102. They used a silicon microsphere resonator for their acoustic storage, where incident laser light detuned from the resonant frequencies could be freely converted to or from the mechanical vibration via a second optical signal. Unlike in Ref. 102, the mechanism here was radiation pressure instead of electrostriction. This means that the storage also allows for conversion between two frequencies of photons. While in principle their storage mechanism preserved not only the amplitude but also full phase information of the entire quantum state of the photons, the thermal background destroyed this coherence in their experiments. This extension was achieved by Verhagen *et al.*[106] with a microring resonator cooled to near the quantum ground state. In addition, they considered the role of their system in optical-to-microwave photon conversion. Palomaki *et al.*[107] extended quantum coherent state transfer to the microwave regime. They used optical waveguide coupled to a superconducting circuit coupled to a mechanical oscillator. This indirect coupling scheme facilitated the control of the coupling between the phonon and photon modes. McGee *et al.*[108] used a mechanical membrane that is metal on one side and dielectric on the other. This allowed them to not only store electrical and optical signals in the phonon modes but also to convert between them. Hill *et al.*[109] used an optical waveguide with regularly spaced pores to store optical photons as phonons and convert them to a second optical frequency. Finally, Galland *et al.*[110] used this approach theoretically analyze the feasibility of storing a single phonon in a mechanical resonant.

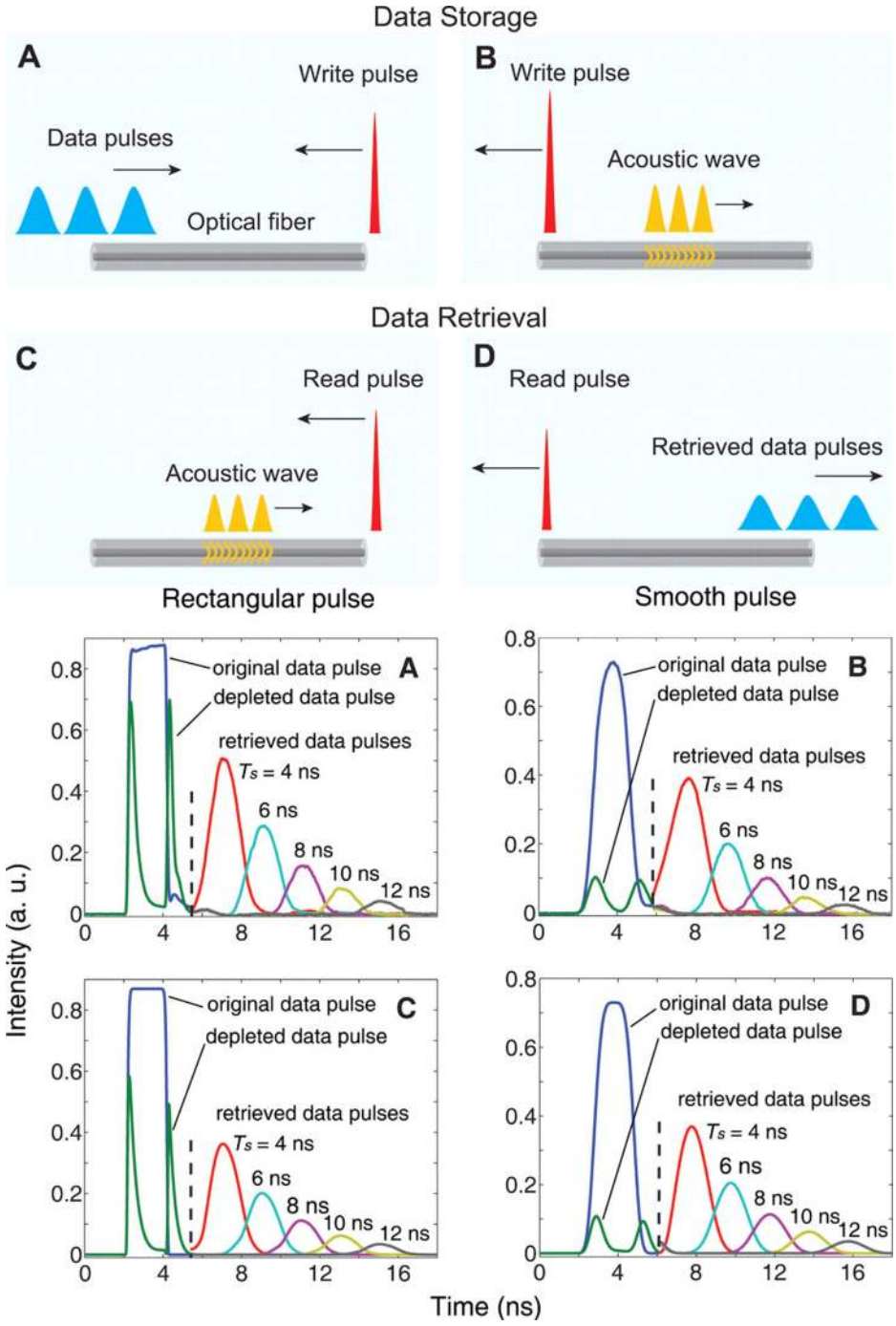

FIG. 10. Optomechanical Memory. (top) Schematic before (A) and after (B) writing and before (C) and after (D) reading. (bottom) Comparison of experiment (A)-(B) vs. theory (C)-(D) for storing and retrieving a rectangular ((A) and (C)) and a smooth ((B) and (D)) pulse. Figure reprinted with permission from Zhu *et al*., Science **318**, 1748 (2007).[102] Copyright 2007 AAAS.

C. Acoustic Storage

In the previous section, phononic storage principally took place through acoustic resonators. The acoustic properties of these systems have been of interest in their own right, principally as a means of evaluating the nature of phonon dissipation. There are a great many forms

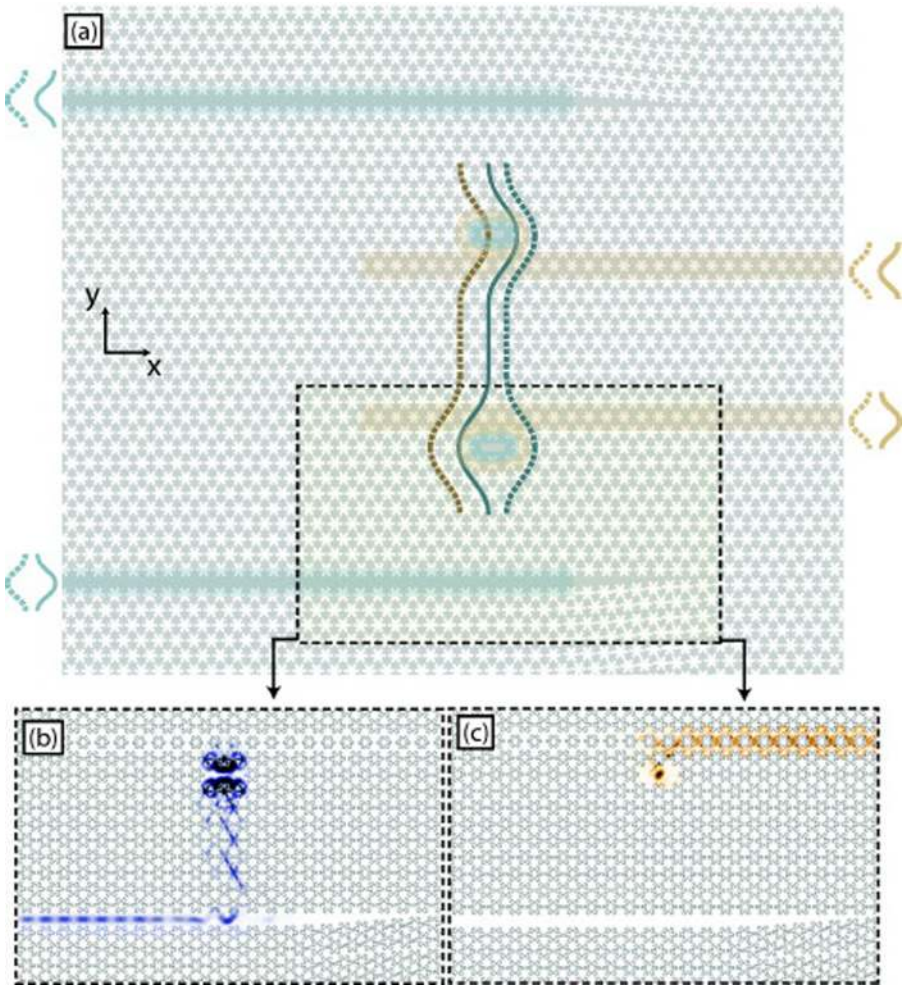

FIG. 11. Optomechanical memory via mode conversion in a phoxonic crystal. (A) Schematic of the phoxonic crystal with optical waveguides (blue) coupled two phononic waveguides (brown) via simultaneous localization to defects. (B) Energy density (Poynting vector) for the photon field. (C) Energy density for the phonon field. Figure from A. H. Safavi-Naeini and O. Painter, New J. Phys. **13**, 013017 (2011).[103]

of phonon dissipation, and understanding and minimizing these loss mechanisms is crucial to construct phononic memory. The direct measure of dissipation in nanoscale resonators was considered by Hill *et al*.[111] They used a series of suspended nanobeams of various lengths as well as torsional rotators (nanobeams with planar structure). By studying the temperature and magnetic field dependence of the dissipation at low temperature, they were able to suss out the many factors responsible for dissipation and isolate the dominant ones. This required them to work to minimize extrinsic loss mechanisms: (1) Purely mechanical effects like clamping (loss induced by strain near the mechanical support), surface roughness, and internal dislocations. (2) Thermal effects like localized heating (often due to Kapitza resistance), thermoelastic loss (coupling of strain to temperature), and thermal expansion. (3) Phonon nonlinearity/anharmonicity (minimized by only using small amplitude phonons) and gas friction (minimized by working in a vacuum). This left intrinsic dissipation as the dominant effect. These are principally due to defects (such as chemical contamination or surface effects) and can take forms like two level systems (transitions between localized defect states) or $D - x$ centers (where donor atoms couple to an unknown defect). They found that the principle form of loss in their system was due to internal defect motion. They also found that surface effects were increasingly important as they reduced system size, a purely nanoscale effect that was not observed in macroscopic resonants due to the difference in surface-to-volume ratio. A notable

feature of acoustic resonators is their exceptionally large quality factors, an important measure of the resilience of the confined phonons against decay. These quality factors tend to fall, however, when working for smaller systems or higher frequencies. Hence, at GHz frequencies, Sun *et al.*[112] find a quality factor of the order 10^3 (principally due to losses through the mechanical support of their microdisk resonator). Meanwhile Goryachev *et al.*[113] work at MHz with a bulk acoustic wave resonator (a high quality crystal slab with curved edges to confine waves to the center of the cell) and find a quality factor of the order 10^9 (at ultralow temperature). And Chakram *et al.*[114] studied a room temperature mesoscale resonator in the MHz and find a quality factor of order 10^7 (principal losses from coupling to the mechanical support). An overview of the various loss mechanisms in a bulk acoustic wave resonator, their functional dependences, and control was given in Goryachev *et al.*[115]

IV. LOGIC

A. Classical Logic

For the most part, phononic logic gates are constructed by the synthesis of various simpler elements. These gates are normally referred to as DDL (diode-diode logic), TTL (transistor-transistor logic), etc. The earliest forms of acoustic logic gates were based upon the concept of phase cancellation. This field was initiated by Owens and Sallee[116] for surface acoustic waves. For example, a NOT gate was created by sending two signals through an interdigital piezoelectric transducer. One signal was a clock signal with predefined frequency and phase. The other was an information carrying signal. When the signal was applied, it would be perfectly out of phase with the clock, and the resulting destructive interference would prevent the transmission of either signal. If the signal were withheld, however, the clock signal would be transmitted without interference. By using combinations of phase differences, they similarly constructed NAND and OR gates. Masmanidas *et al.*[117] independently developed a similar approach many years later. They used a pair of piezoelectric NEM cantilevers joined to each other at right angles. Each cantilever was independently driven by an AC signal of the same frequency but opposite phase. If only one signal was applied the cantilevers would oscillate, but if both were applied the destructive interference would eliminate the oscillation. They used this effect to construct an XOR gate and did not concern themselves with other logic gates. The approach of Owens and Sallee was fully updated in Bringuier *et al.*,[118] who used a PC to increase the versatility of the phase cancellation. Specifically, they exploit the fact that waves approaching from two different angles can be mapped onto the same point in the Brillouin zone, thereby controlling the phase each will acquire in passing through the PC. Once they leave the PC the waves will diverge, resulting in beam splitting. However, the two beams can still interfere with each other, giving destructive interference at particular points. If a detector were placed at the location of destructive interference, then the logic gates will work similar to before. Each input will have an input and a fixed reference. Applying the input will induce destructive interference at the detector, as in a NOT gate (see Fig. 12). Using two different inputs with two in phase reference signals gives a NAND gate. Using two different inputs with two out of phase reference signals gives an XOR gate. For these gates any arbitrary classical logic function can be constructed. Further, the use of a PC makes this interference based computing architecture more compact and more readily adapted to a range of input angles than previous approach.

Thermal logic gates were taken up in Wang and Li,[119] using their work on thermal transistors.[70,71] In that setup, the transistor was constructed of three nonlinear 1D lattices joined to each other to form a T-shape. They find that, when changing the temperature at the gate, NDTR between the gate/source gives a great deal of control of the temperature at the drain. While in their previous work they examined the temperature at the far end of the drain, here they look at the near end (i.e. closest to the junction), where NDTR results in a drop in temperature across the boundary as a function of increasing gate temperature. However, this drop is insufficient to bring the temperature from logical 1 (high temperature) to logical 0 (low temperature). To accomplish this, they connect this end of the drain to a temperature divider (in analogy with a voltage divider), using the difference of thermal impedances to tune the resultant temperature. Using NDTR and the temperature divider,

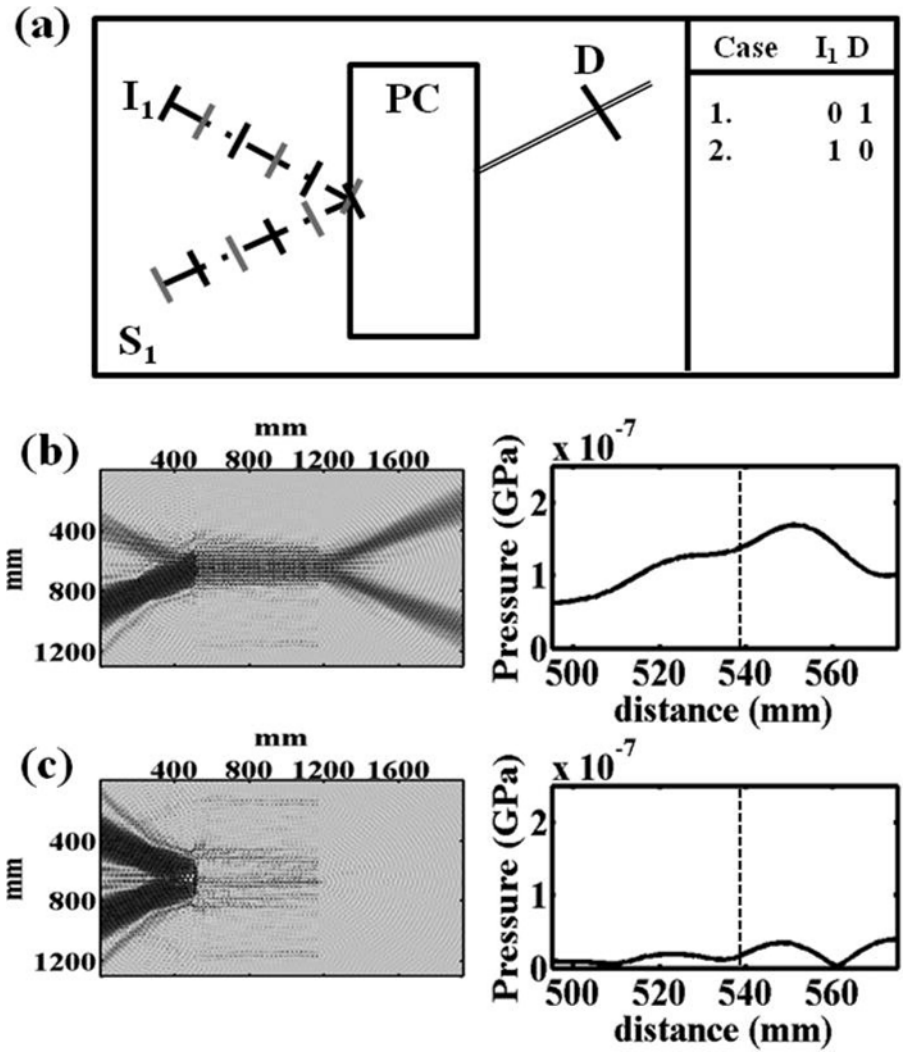

FIG. 12. Operation of a NOT gate. (A) Schematic layout of input I, source S, and detector D as well as truth table. (B) Simulated intensity when no signal is applied from input I. (C) Simulated intensity when a signal is applied from input I. Figure reprinted with permission from Bringuier *et al.*, J. Acoust. Soc. Am. **130**, 4 (2011).[118] Copyright 2011 Acoustic Society of America.

they are able to construct a thermal NOT gate (high temperature yields low temperature and vice versa). They also demonstrate that this set-up works similar to a repeater – temperatures above or below a cut-off are each mapped to a fixed temperature (in an ideal repeater, their setup require several repeaters in series to achieve this effect). If these repeaters are tuned to produce specific temperature profiles, then they can in turn construct AND and OR gates.

Another extension of an existing design to logic was developed in the supplementary materials of Boechler *et al.*[62] There, they used a defect in a nonlinear granular crystal to convert a normally blocked signal into a transmitted one. For the nonlinearity to be effective, it was necessary that the amplitude exceed some critical value. If there are two inputs which are both too small for this critical driving, but whose sum is sufficient, then an AND gate can be constructed. On the other hand, an OR gate can be constructed by using inputs connected to two branches of the lattice, each with a defect. If either input is above the critical value then a signal will be transmitted. One limitation of this approach, however, is that there is no obvious way to construct a NOT gate. Li *et al.*[78] tackled this construction of logic from a granular crystal using the granular transistor (unlike the previous work, which used a granular rectifier). So instead of requiring a defect, this setup

had a pair of signals whose nonlinear interaction sufficed to induce transmission of a current in the band gap. They follow Mahboob *et al.*[120] (see the following section) and use three signals of incommensurate frequency (i.e. no $f_a \neq nf_b + mf_c$ for any rational n,m). Two of the signals are low frequency (below the band gap), and one is high frequency (above the band gap). The nonlinear interaction of the two low-frequency signals creates a high frequency signal (at an incommensurate frequency) in the band gap, thus creating a detectable AND signal. The nonlinear interaction of either low frequency signal with the high frequency one will induce the transmission of the high frequency signal, thus serving as a detectable OR signal. To create a NOT gate, it is necessary to add additional signals at the two low frequencies. These signals need to be out of phase with the previous ones, creating destructive interference (as in Refs. 116–118).

B. Classical Logic Beyond the Diode/Transistor Framework

The development of wave-based phonon logic opens up several interesting avenues in nonlinear information processing. Mahboob *et al.*[120] developed an approach to frequency-domain parallel computing based upon a single NEM resonantor. While the use of frequency domain multiplexing (i.e. the simultaneous transmission of information over multiple frequencies) is a common approach in conventional computing, applying logic gates to a multiplexed signal remains difficult. In practice, it is often preferable to demultiplex an electronic signal (say, by using a series of filters to select out different frequencies), act on each separately, and then recombine them. This problem is eliminated here though, by means of nonlinear interactions. Specifically, they use a piezoelectric mechanical resonator attached to electrical contacts. One of these contacts is a 2D electron gas, which is driven (initially) at twice the fundamental frequency of the NEM resonator to input information (they term this the pump, in analogy with parametric amplification). Directly above the electron gas is another electrical input, this one driven (initially) at precisely the fundamental mode (which they term the signal) (see Fig. 13(a)). The signal is able to excite mechanical motion, but the pump is too weak to do so. Allowing the pump/signal to drift from these frequencies results in new frequencies being excited (principally at the different of the two). It is these new frequencies that allow the detection of various logic operations (see Fig. 13(b)). To create an AND gate, two pump inputs are applied/withheld (at $2f_0 \pm \Delta$, where f_0 is the fundamental mode) while the signal is driven at $f_0 - \delta$. The interaction of these signals creates new ("idler") modes at the frequency differences ($f_0 \pm \Delta - \delta$) as well as second order interactions at $f_0 \pm 2\Delta + \delta$. These second order idler modes can only be present if both inputs are active, and so are indicative of an AND operation (see Fig. 13(c)). To create an OR gate, two signal inputs at $f_0 \pm \Delta + \delta$ are applied along with pump inputs as before. Either pump input can excite an $f_0 - \delta$ mode, which indicates an OR operation. Further, the OR operation can yield XOR if the relative phase of the $f_0 - \delta$ signals result in destructive interference (see Fig. 13(d)). While the authors then argue that AND, OR, and XOR are sufficient for all classical logic operations, this is only true if there is also a NOT gate. This can only be accomplished if one of the inputs in the XOR gate is fixed (compare to Refs. 116 and 117). Because the each logic output requires a separate frequency, fixing some frequency inputs is a notable limitation of this approach. On the other hand, this approach allows for all 2^{N+1} N-bit logic operations to in principle be performed on the same circuit element. This constitutes a significant reduction in circuit size and increase in parallel information processing.

Sklan and Grossman[121] independently developed a nonlinear parallel processing approach based on magneto-acoustics. As before,[11] they used horizontally and vertically polarized transverse phonons as their logical 0 and logical 1 at a given frequency (as opposed to the presence or absence of a current). They construct logic elements from 90° Faraday rotators (aka gyrator). These rotators can either be fixed or they can be controlled by the detection of a vertically polarized signal (rotation present if the signal is detected or suppressed if no signal is detected, as in the transistor configuration in Ref. 11). In this framework, a NOT gate a controlled rotator followed by a fixed rotator. If the controlled rotator is active (logical 1 applied to the gate) then the two rotations combine to become a 180° rotation, just a change of sign of the logical 0 signal moving from source to drain. On the other hand, if the rotator is inactive (logical 0 applied to the gate) then logical 0 at the source becomes logical 1 at the drain. For an OR gate, two signals are allowed to non-destructively superimpose

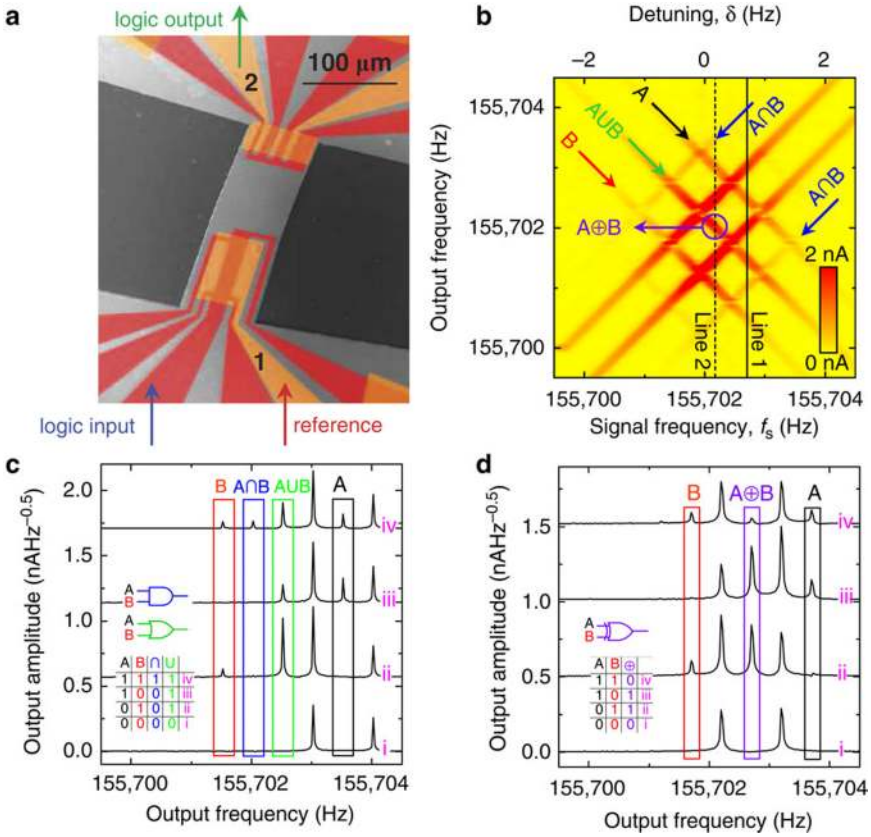

FIG. 13. Diode and transistor free logic. (A) Schematic of the NEM resonator. (B) Frequency diagram. Input frequencies for the two pump signals (purple arrow in (A)) form the A and B inputs, while the reference signals f_s (red arrow in (A)) is allowed to vary. Curves splitting off from the main diagonal are the logic outputs (green arrow in (A)), with different interaction peaks corresponding to AND (blue), OR (green), and XOR (purple). (C)-(D) Output amplitude for fixed signal frequency, going along the solid (C) and dashed (D) black lines of (B). Figure adapted with permission from Mahboob *et al.*, Nat. Commun. **2**, 198 (2011).[120] Copyright 2011 Macmillan Publishers Ltd: Nature.

at the control of a single rotator. If either signal is present, it will exceed the threshold to activate the rotator. Using a combination rotators controlled by the sum of two signals or a single signal and fixed rotators, they construct all the 2-terminal logic gates. They then extend this to parallel logic by considering a set of inputs at different frequencies. They show that the rotators can be constructed as a composite of several smaller rotators in such a way that a 90° rotation is applied at one frequency and no rotation is found at another. Thus, rotators can be activated for different frequencies, allowing for different logic operations to be applied within the same basic circuit. While this parallelization is similar to Ref. 120, in that approach the number of frequencies grows exponentially with the number of inputs while the logic gate remains equally complex. In Ref. 121, the number of frequencies grows linearly with the number of inputs but the logic gate's complexity grows quadratically.

C. Quantum Computing

Optomechanics and nanoelectromechanics have been considered as avenues of quantum computing. In general, though, these approaches have used photonic or superconducting qubits, with the phononic elements only entering for storage (see the Memory section for more detail). Stannigel *et al.*[122] take this approach initially. They use a pair of multimode optomechanical channels where low frequency optical mode couplings are used for converting photons to or from the phononic memory (a linear operation) and high frequency optical mode couplings were used to perform nonlinear

gate operations on photons. In addition, they used the optomechanical coupling to construct a photon transistor where the interaction is mediated by phonon modes. More significantly, they also considered gate operations between two phonons generated by their joint interaction with a common optical mode. By changing the strength of the optical mode (i.e. its classical amplitude), the nonlinearity of the phonon-phonon interaction was tunable. Schmidt *et al.*[123] focused on the case where information was stored in phononic modes and optomechanical interactions were used to control the interactions between the modes. They consider an optomechanical crystal as their model system, where phonon modes are confined to various cavities within the crystal. The phonon modes are all in contact with an optical mode (i.e. a laser). The interaction of the photon and phonon modes induces an effective coupling between phonon modes, itself tunable by the strength of the optical field. Depending upon the frequencies present in the laser, the optical field can swap phonons between modes when the optical frequency equals half the difference of phonon frequencies ($2\omega = \Omega_i - \Omega_j$ where ω is the optical frequency, Ω_i the phonon frequency of mode i, J the effective phonon-phonon coupling strength, and b the phonon destruction operator). Additionally, the optical field can entangle phonons when the optical driving frequency is the average of two phonon modes $2\omega = \Omega_i + \Omega_j$. Finally, when the photon and phonon modes are resonan ($\omega = \Omega_i$), the optical field will drive the phonons into a squeezed mode. The strength of effective photon-phonon coupling needs to be balanced between operational mixing (e.g. unwanted swapping) at high power and thermalization/decay at low power. To aid the convenient realization of this system, they consider a series of phonon modes within a confined frequency range as constituting their memory, as well as a set of high frequency auxiliary modes for accessing the memory. Thus, entangling two modes is possible by swapping them into the auxiliaries (a low frequency operation), entangling them (a high frequency operation), and then swapping them back (see Fig. 14). This gives them an architecture for scalable coherent nanomechanical state processing.

The NEM resonator approach to phononic quantum computing was considered by Rips and Hartmann.[124] They use an array of doubly clamped nanobeams coupled to a resonant mode of an optical cavity. Each beam is also individually addressable via contact with an array of electrodes, which are used to tune the anharmonicity of the beams until only a single transition channel is feasible by optical coupling (i.e. each beam behaves like a two level system and therefore like a binary qubit). Single qubit gates are constructed from the Pauli spin basis ($\sigma_x, \sigma_y, \sigma_z$), which they generate by applying radio-frequency electric fields from the electrode tips. V_z generates a σ_z rotation and $V_{x,y}$ generate linear combinations of σ_x, σ_y (decoupled for purely horizontal or vertical fields). Two qubit are constructed from the interaction with the optical cavity. Two qubits are detuned to have a common transition frequency, distinct from the transition frequencies of the other qubits. As in Ref. 123, the effective interaction of the phonons via the photon field induces hopping between sites, which they use to create a fundamental entangling gate – the ISWAP gate.

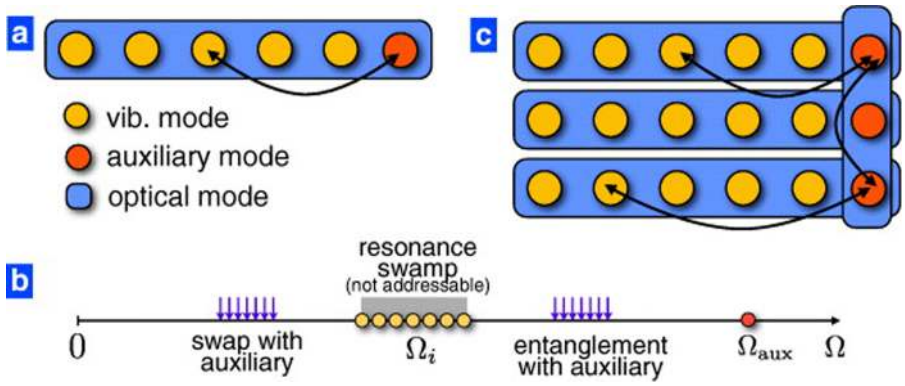

FIG. 14. Optomechanical phononic quantum computing. (A) Single optical cavity (blue) with one directly addressable auxilary phonon mode (orange) and multiple indirectly accesible phonon modes (yellow). (B) Frequency diagram. Low frequency signals induce a hopping interaction between particulay phonon modes and the auxiliary mode, while high frequency modes entangle particular phonon modes with the auxiliary. (C) Protocol to entangle two phonon modes in different optical cavities. Figure from M. Schmidt, M. Ludwig, and F. Marquardt, New J. Phys. **14**, 125005 (2012).[123]

Specifically, the optical coupling generates $\sqrt{\pm\text{ISWAP}}$. Applying $\sqrt{\text{ISWAP}}$ between two qubits, a π rotation about z on the first qubit, $\sqrt{-\text{ISWAP}}$ (i.e. the inverse of the first operation), and finally a $-\pi$ rotation about z on the same qubit will entangle the desired pair while leaving the others unaffected. These elements together at least conceptually constitute a quantum computer, the feasibility of which they examine numerically. Faust *et al.*[125] took a somewhat different approach to a NEMs qubit and sought to construct a purely classical to level system that could be used for modeling quantum two level systems. Their system consisted of a pair of nanomechanical resonators with coupled flexural modes. The coupling was generated via a voltage bias on each NEM resonator, creating an electric potential difference between them. The system was further tuned by means of a constant voltage bias to bring the energy levels of the flexural modes near their avoided crossing. Okamoto *et al.*[126] simultaneously studied the use of phonons in NEM resonators for classical two level systems and quantum qubits. They also use an electrically coupled pair of NEM beam resonators, but unlike the linear coupling in Ref. 125, their coupling is parametric and can switch between linear and nonlinear. They exploit this nonlinearity to induce classical multi-wave phonon mixing between the two resonators, and consider extensions of their technique to the high frequency, quantum mechanical regime.

An alternative approach to quantum circuit elements is developed in Soykal *et al.*[127] and refined in Ruskov and Tahan[128]. Specifically, they consider localized phonon mode coupled to an impurity to create a phoniton. In Ref. 127 they used a donor defect within a strained silicon cavity, while in Ref. 128 they used an acceptor defect on a patterned silicon nanomembrane (the properties of which they tune using a magnetic field and electric field/strain). Here, phonons are principally used as a (strain, electric field) tunable coupling with the phoniton qubit. In particular, phonons can be used to modify (via Rabi oscillations) or read the state of the qubit (the phonons then likely being read optically). So unlike in previous designs, where the phonon modes were used to store information and photons were used to access it, here information is principally stored electronically and then accessed via phonons (with the quasiparticle phoniton as the means of interaction).

V. CONCLUSIONS

Having examined each aspect of phononic information processing, it is worth reconsidering the question of what potential role phononic computing might play. Some parts of the phononic computing architecture have applications in their own right. Acoustic rectifiers have the potential to remove noise, reduce injuries, and improve the performance of ultrasound.[39] Thermal rectifiers have potential applications in thermal insulation and nanoscale thermal management.[129] Thermal memory is intimately related to questions of heat storage for energy and heating applications.[91–93] As an information processing architecture, though, the sheer diversity of approaches to phononic computing makes generalization difficult. Nanoscale mechanical resonator systems have proven particularly useful given their low power consumption.[8] The combination of Moore's Law exponentially increasing transistor density (and thereby computing capacity) and the Landauer limit to the energy required for computation means that power consumption and management by conventional electronics is of increasing concern. (A similar concern exists for photonic computers, as reducing feature size in such photonic systems increases the power needed to overcome shot noise). The lower power cost of mechanical circuits is therefore a potentially important application, but one that comes at a cost of slower response times than conventional computing. While this is a formidable challenge for future research, there are also innovative approaches to try to circumvent this problem. The use of unconventional, frequency-domain parallelization (as in Refs. 120 and 121) has the potential to increase the number of operations per second even as the speed of each operation falls below the electronic transistor's speed. This gives phononic computing a potential advantage in situations where highly parallelized computation is important, which is also the regime where power consumption and dissipation are particular worries. Thus, low power, high throughput computation holds unique opportunities for phononic computing. A second case where low power computation leads to novel and important opportunities is in the exploitation of naturally occurring power sources and parasitic losses. The ability to convert wasted heat and

parasitic vibrations into intelligible information could potentially herald new applications. Ambient systems incorporating sound[130] and heat in gases or liquids could be made "smart" in a way that is difficult to accomplish with electronic devices (as water tends to short circuit electronics). Particularly notable is the use of trees to construct phononic crystals in Ref. 130, which suggests the possibility of incorporating information processing power into the environment in a far more innocuous, environmentally-friendly method than other computing architectures (save perhaps biological computing). Moreover, nanomechanical and thermal systems can potentially operate in a wider range of temperatures than silicon based electronics. In quantum computing, phonons offer further advantages. Their relatively long lifetimes have made them an intriguing option for memory. Furthermore, their ready coupling to a wide range of systems means that they can potentially translate between multiple quantum computing architectures. This has the potential to allow for a hybrid quantum computer, where the advantages of different implementations are combined to compensate for each other's weaknesses. This approach may constitute one the most promising frameworks for a practical implementation of quantum computing, and is an approach uniquely suited to phonons ready coupling to multiple systems. As a stand-alone realization of quantum computing, phonons are in a more ambiguous situation. While there are certainly scenarios with long phonon lifetimes, the need for nonlinearity in the construction of two-phonon gates makes the elimination of losses difficult. On the other hand, phonons interact with each other more readily than photons and can be used for traveling waves and standing waves (memory). They can thus be localized and interact with each other more easily than photons, while still supporting the ready transfer of information in the form of traveling waves. Furthermore, the wave nature of phonons can be observed over longer length scales than electrons, and their bosonic symmetry may make the preparation of large populations in a particular quantum state more tractable than for fermions.

Significant issues remain for phononic computing, however. While parity-breaking rectifiers have been studied extensively, the breadth of the field (for realizations, the source of the rectification effect, and the fundamental nature of rectification) means that there are still open questions for both theorists and experimentalists.[12–14] Some of these challenges could be answered by moving from an enumeration of theoretical mechanisms of linear, reciprocal rectification (and its amplification), to developing more device or application designs incorporating these effects. After all, the most fundamental criticism of this topic is not that these funneling effects don't exist, but that they are trivial and lacking in utility. The problems facing the parity-breaking rectifiers are also partially the result of the tight focus on this problem to the exclusion of others. While problems in parity-breaking rectifiers remain open to further study, studies of other aspects of phononic computing are even less developed. Most work on phononic memory and NEMs computers has presumed an electronic or photonic information carrier, with little attention paid to purely phononic memory. Similar, rectification of phonons through the breaking of time-reversal symmetry (as well as $\mathcal{PT}$ symmetry) and dynamical control of phonons robust enough to create phononic transistors are topics that are only beginning to receive attention. Experimental study of the many theoretical implementations discussed here is sorely needed, as is increased theoretical attention towards experimentally realizable systems. Still, the promise of phononic devices for information processing and energy management suggests that further work in phononic computing has the potential for great fundamental and practical rewards.

ACKNOWLEDGMENTS

The author thanks J. Grossman, A. Maznev, and C. Sotomayor for their helpful discussion and suggestions. This material is based upon work supported by the National Science Foundation Graduate Research Fellowship under Grant No. 1122374.

[1] T. Freeth, Y. Bitsakis, X. Moussas, J. H. Seiradakis, A. Tselikas, E. Mankou, M. Zafeiropulou, R. Hadland, D. Bate, A. Ramsey, M. Allen, A. Crawley, P. Hockley, T. Malzbender, D. Gelb, W. Ambrisco, and M. G. Edmunds, Nature **444**, 7119 (2006).
[2] B. Pascal, *Oeuvres de Blaise Pascal* (La Haye, Chez Detune, 1779).
[3] D. De and S. Price, IEEE Micro. **4**, 1 (1984).
[4] N. Sharkey, "A programmable robot from 60 AD 2611," New Sci. **2611** (2007).
[5] G. Brett, Speculum **29**, 3 (1954).

[6] D. Swade, *Charles Babbage's Difference Engine No. 2 Technical Description* (Science Museum Papers in the History of Technology No 5, London: National Museum of Science and Industry, 1996).
[7] J. Fuegi and J. Francis, Ann. Hist. Comput. **25**, 4 (2003).
[8] M. L. Roukes, Electron Devices Meeting, IEDM Technical Digest. 539 (2004).
[9] M. Maldovan, Nature **503**, 209 (2013).
[10] We will neglect the applications of phonons to problems like time-keeping through quartz resonator mechanical clocks and the use of surface acoustic waves in thin film resonators for signal filtering and convolution. While these are undoubtedly useful for computing, they are somewhat ancillary. In particular, they fall outside of the Turing machine framework for a computer.
[11] S. R. Sklan and J. C. Grossman, New J. Phys. **16**, 053029 (2014).
[12] A. A. Maznev, A. G. Every, and O. B. Wright, Wave Motion **50**, 776 (2013).
[13] N. Li, J. Ren, L. Wang, G. Zhang, P. Hänggi, and B. Li, Rev. Mod. Phys. **84**, 1045 (2012).
[14] N. A. Roberts and D. G. Walker, Int. J. Therm. Sci. **50**, 648 (2011).
[15] C. Starr, J. Appl. Phys. **7**, 15 (1935).
[16] A. M. Clausing, Int. J. Heat Mass Tran. **9**, 791 (1966).
[17] M. H. Barzelay, K. N. Tong, and G. F. Holloway, *Joints Technical Report 3295* (NACA, 1955).
[18] D. V. Lewis and H. C. Perkins, Int. J. Heat Mass Tran. **11**, 1371 (1968).
[19] M. Sen and D. Go, J. Heat Transf. **132**, 124502 (2010).
[20] C. Dames, J. Heat Transf **131**, 061301 (2009).
[21] W. Kobayashi, Y. Teraoka, and I. Terasaki, Appl. Phys. Lett. **95**, 171905 (2009).
[22] T. Sun, J. Wang, and W. Kang, EPL-Europhys. Lett. **105**, 16004 (2014).
[23] M. Romero-Bastida and J. M. Arizmendi-Carvajal, J. Phys. A: Math. Theor. **46**, 115006 (2013).
[24] J. Lee, V. Varshney, A. K. Roy, J. B. Ferguson, and B. L. Farmer, Nano Lett. **12**, 3491 (2012).
[25] Y. Wang, A. Vallabhaneni, J. Hu, B. Qiu, Y. P. Chen, and X. Ruan, Nano Lett. **14**, 592 (2014).
[26] C. W. Chang, D. Okawa, A. Majumdar, and A. Zettl, Science **314**, 1121 (2006).
[27] A. A. Balandina and D. L. Nika, Mater. Today **15**, 6 (2012).
[28] M. Alaghemandi, F. Leroy, E. Algaer, M. Bohm, and F. Muller-Plathe, Nanotechnology **21**, 075704 (2010).
[29] E. Pereira, Phys. Rev. E **83**, 031106 (2011).
[30] M. Terraneo, M. Peyrard, and G. Casati, Phys. Rev. Lett. **88**, 094302 (2002).
[31] B. Li, L. Wang, and G. Casati, Phys. Rev. Lett. **93**, 184301 (2004).
[32] B. Hu, L. Yang, and Y. Zhang, Phys. Rev. Lett. **97**, 124302 (2006).
[33] J. Lan, L. Wang, and B. Li, Int. J. Mod. Phys. B **21**, 4013 (2007).
[34] T. Komatsu and N. Ito, Phys. Rev. E **81**, 010103(R) (2010).
[35] W. Kobayashi, D. Sawaki, T. Omura, T. Katsufuji, Y. Moritomo, and I. Terasaki, Appl. Phys. Express **5**, 027302 (2012).
[36] M. Peyrard, EPL-Europhys. Lett. **76**, 1 (2006).
[37] K. I. Garcia-Garcia and J. Alvarez-Quintana, Int. J. Therm. Sci. **81**, 76 (2014).
[38] B. Li, J. H. Lan, and L. Wang, Phys. Rev. Lett. **95**, 104302 (2005).
[39] S. Zhu, T. Dreyer, M. Liebler, R. Riedlinger, G. M. Preminger, and P. Zhong, Ultrasound Med. Biol. **30**, 5 (2004).
[40] R. Krishnan, S. Shirota, Y. Tanaka, and N. Nishiguchi, Solid State Commun. **144**, 194 (2007).
[41] S. Danworaphong, T. A. Kelf, O. Matsuda, M. Tomoda, Y. Tanaka, N. Nishiguchi, O. B. Wright, Y. Nishijima, K. Ueno, S. Juodkazis, and H. Misawa, Appl. Phys. Lett. **99**, 201910 (2011).
[42] S. Alagoz, Appl. Acoust. **76**, 402 (2014).
[43] M. Schmotz, J. Maier, E. Scheer, and P. Leiderer, New J. Phys. **13**, 113027 (2011).
[44] H.-X. Sun, S.-Y. Zhang, and X.-J. Shui, Appl. Phys. Lett. **100**, 103507 (2012).
[45] H. Jia, M. Ke, C. Li, C. Qiu, and Z. Liu, Appl. Phys. Lett. **102**, 153508 (2013).
[46] H.-X. Sun and S.-Y. Zhang, Appl. Phys. Lett. **102**, 113511 (2013).
[47] X. Zhu, X. Zou, B. Liang, and J. Cheng, J. Appl. Phys. **108**, 124909 (2010).
[48] Depending upon whether the background medium is a solid or a gas/liquid, phononic crystals will often be divided between phononic and sonic crystals. To emphasize the similarity between these cases, I refer to both as phononic crystals in this paper.
[49] R.-Q. Li, B. Liang, Y. Li, W.-W. Kan, X.-Y. Zou, and J.-C. Cheng, Appl. Phys. Lett. **101**, 263502 (2012).
[50] J.-J. Chen, X. Han, and G.-Y. Li, J. Appl. Phys. **113**, 184506 (2013).
[51] J. Lu, C. Qiu, M. Ke, and Z. Liu, arXiv:1411.1851 (2014).
[52] B. Yuan, B. Liang, J.-C. Tao, X.-Y. Zou, and J.-C. Cheng, Appl. Phys. Lett. **101**, 043503 (2012).
[53] A. Cicek, O. A. Kaya, and B. Ulug, Appl. Phys. Lett. **100**, 111905 (2012).
[54] B. Liang, B. Yuan, and J.-C. Cheng, Phys. Rev. Lett. **103**, 104301 (2009).
[55] B. Liang, X.-Y. Zou, B. Yuan, and J.-C. Cheng, Appl. Phys. Lett. **96**, 233511 (2010).
[56] B. Liang, X. S. Guo, J. Tu, D. Zhang, and J. C. Cheng, Nat. Mater. **9**, 989 (2010).
[57] X. Guo, Z. Lin, J. Tu, B. Liang, J. Cheng, and D. Zhang, J. Acoust. Soc. Am. **133**, 2 (2013).
[58] C. Ma, R. G. Parker, and B. B. Yellen, J. Sound Vib. **332**, 4876 (2013).
[59] S. Lepri and G. Casati, Phys. Rev. Lett. **106**, 164101 (2011).
[60] T. F. Assunção, E. M. Nascimento, and M. L. Lyra, Phys. Rev. E **90**, 022901 (2014).
[61] N. Li and J. Ren, arXiv:1402.5576 (2014).
[62] N. Boechler, G. Theocharis, and C. Daraio, Nat. Mater. **10**, 665 (2011).
[63] A. Merkel, V. Tournat, and V. Gusev, Phys. Rev. E **90**, 023206 (2014).
[64] S. Lepri and A. Pikovsky, Chaos **24**, 043119 (2014).
[65] R. Fleury, D. L. Sounas, C. F. Sieck, M. R. Haberman, and A. Alù, Science **343**, 516 (2014).
[66] J. D'Ambroise, P. G. Kevrekidis, and S. Lepri, J. Phys. A: Math. Theor. **45**, 444012 (2012).

[67] X. Zhu, H. Ramezani, C. Shi, J. Zhu, and X. Zhang, Phys. Rev. X **4**, 031042 (2014).
[68] M. B. Zanjani, A. R. Davoyan, A. M. Mahmoud, N. Engheta, and J. R. Lukes, Appl. Phys. Lett. **104**, 081905 (2014).
[69] B.-I. Popa and S. A. Cummer, Nat. Commun. **5**, 3398 (2014).
[70] B. Li, L. Wang, and G. Casati, Appl. Phys. Lett. **88**, 143501 (2006).
[71] W. C. Lo, L. Wang, and B. Li, J. Phys. Soc. Japan **77**, 054402 (2008).
[72] T. S. Komatsu and N. Ito, Phys. Rev. E **83**, 012104 (2011).
[73] S. Alagoz and B. B. Alagoz, J. Acoust. Soc. Am. **133**, 6 (2013).
[74] D. Hatanaka, I. Mahboob, K. Onomitsu, and H. Yamaguchi, Appl. Phys. Lett. **102**, 213102 (2013).
[75] D. Hatanaka, I. Mahboob, K. Onomitsu, and H. Yamaguchi, Nat. Nanotechnol. **9**, 520 (2014).
[76] C. Vanhille and C. Campos-Pozuelo, Ultrason. Sonochem. **21**, 50 (2014).
[77] B. Liang, W.-W. Kan, X.-Y. Zou, L.-L. Yin, and J.-C. Cheng, Appl. Phys. Lett. **105**, 083510 (2014).
[78] F. Li, P. Anzel, J. Yang, P. G. Kevrekidis, and C. Daraio, Nat. Commun. **5**, 5311 (2014).
[79] F. Li, C. Chong, J. Yang, P. G. Kevrekidis, and C. Daraio, arXiv: 1408.6121 (2014).
[80] V. F. Nesterenko, C. Daraio, E. B. Herbold, and S. Jin, Phys. Rev. Lett. **95**, 158702 (2005).
[81] X.-F. Li, X. Ni, L. Feng, M.-H. Lu, C. He, and Y.-F. Chen, Phys. Rev. Lett. **106**, 084301 (2011).
[82] K. G. S. H. Gunawardana, K. Mullen, J. Hu, Y. P. Chen, and X. Ruan, Phys. Rev. B **85**, 245417 (2012).
[83] M. G. Menezes, A. Saraiva-Souza, J. Del Nero, and R. B. Capaz, Phys. Rev. B **81**, 012302 (2010).
[84] H. Jeong, Y. D. Jho, and C. J. Stanton, arXiv: 1408.4731 (2014).
[85] J. Zhu, K. Hippalgaonkar, S. Shen, K. Wang, J. Wu, X. Yin, A. Majumdar, and X. Zhang, arXiv:1307.4069 (2013).
[86] P. Ben-Abdallah and S.-A. Biehs, Phys. Rev. Lett. **112**, 044301 (2014).
[87] S. R. Sklan and J. C. Grossman (in preparation).
[88] M. V. Wilkes, J. ACM **15**, 1 (1968).
[89] L. Wang and B. Li, Phys. Rev. Lett. **101**, 267203 (2008).
[90] R. Xie, C. T. Bui, B. Varghese, Q. Zhang, C. H. Sow, B. Li, and J. T. L. Thong, Adv. Funct. Mater. **21**, 1602 (2011).
[91] A. Sharma, V. V. Tyagi, C. R. Chen, and D. Buddhi, Renew. Sust. Energ. Rev. **13**, 318 (2009).
[92] J. M. Khodadadi, L. Fan, and H. Babaei, Renew. Sust. Energ. Rev. **24**, 418 (2013).
[93] M. Fasano, M. B. Bigdeli, M. R. V. Sereshk, E. Chiavazzo, and P. Asinari, Renew. Sust. Energ. Rev. **41**, 1028 (2015).
[94] T. Rueckes, K. Kim, E. Joselevich, G. Y. Tseng, C.-L. Cheung, and C. M. Lieber, Science **289**, 94 (2000).
[95] A. N. Cleland and M. R. Geller, Phys. Rev. Lett. **93**, 070501 (2004).
[96] P. Rabl, S. J. Kolkowitz, F. H. L. Koppens, J. G. E. Harris, P. Zoller, and M. D. Lukin, Nat. Phys. **6**, 602 (2010).
[97] R. L. Badzey, G. Zolfagharkhani, A. Gaidarzhy, and P. Mohanty, Appl. Phys. Lett. **85**, 3587 (2004).
[98] W. J. Venstra, H. J. R. Westra, and H. S. J. van der Zant, Appl. Phys. Lett. **97**, 193107 (2010).
[99] N. A. Khovanova and J. Windelen, Appl. Phys. Lett. **101**, 024104 (2012).
[100] I. Mahboob and H. Yamaguchi, Nat. Nanotechnol. **3**, 275 (2008).
[101] I. Mahboob, M. Mounaix, K. Nishiguchi, A. Fujiwara, and H. Yamaguchi, Sci. Reports **4**, 4448 (2014).
[102] Z. M. Zhu, D. J. Gauthier, and R. W. Boyd, Science **318**, 1748 (2007).
[103] A. H. Safavi-Naeini and O. Painter, New J. Phys. **13**, 013017 (2011).
[104] D. E. Chang, A. H. Safavi-Naeini, M. Hafezi, and O. Painter, New J. Phys. **13**, 023003 (2011).
[105] V. Fiore, Y. Yang, M. C. Kuzyk, R. Barbour, L. Tian, and H. Wang, Phys. Rev. Lett. **107**, 133601 (2011).
[106] E. Verhagen, S. Deleglise, S. Weiss, A. Schliesser, and T. J. Kippenberg, Nature **482**, 63 (2012).
[107] T. A. Palomaki, J. W. Harlow, J. D. Teufel, R. W. Simmonds, and K. W. Lehnert, Nature **495**, 210 (2013).
[108] S. A. McGee, D. Meiser, C. A. Regal, K. W. Lehnert, and M. J. Holland, Phys. Rev. A **87**, 053818 (2013).
[109] J. T. Hill, A. H. Safavi-Naeini, J. Chan, and O. Painter, Nat. Commun. **3**, 1196 (2012).
[110] C. Galland, N. Sangouard, N. Piro, N. Gisin, and T. J. Kippenberg, Phys. Rev. Lett. **112**, 143602 (2014).
[111] P. Mohanty, D. A. Harrington, K. L. Ekinci, Y. T. Yang, M. J. Murphy, and M. L. Roukes, Phys. Rev. B **66**, 085416 (2002).
[112] X. Sun, X. Zhang, and H. X. Tang, Appl. Phys. Lett. **100**, 173116 (2012).
[113] M. Goryachev, D. L. Creedon, E. N. Ivanov, S. Galliou, R. Bourquin, and M. E. Tobar, Appl. Phys. Lett. **100**, 243504 (2012).
[114] S. Chakram, Y. S. Patil, L. Chang, and M. Vengalattore, Phys. Rev. Lett. **112**, 127201 (2014).
[115] M. Goryachev, M. E. Tobar, and S. Galliou, *IEEE Joint UFFC, EFTF and PFM Symposium* (2013).
[116] J. M. Owens and G. F. Sallee, Proc. IEEE **159**, 308 (1971).
[117] S. C. Masmanidis, R. B. Karabalin, I. De Vlaminck, G. Borghs, M. R. Freeman, and M. L. Roukes, Science **317**, 780 (2007).
[118] S. Bringuier, N. Swinteck, J. O. Vasseur, J.-F. Robillard, K. Runge, K. Muralidharan, and P. A. Deymier, J. Acoust. Soc. Am. **130**, 4 (2011).
[119] L. Wang and B. Li, Phys. Rev. Lett. **99**, 177208 (2007).
[120] I. Mahboob, E. Flurin, K. Nishiguchi, A. Fujiwara, and H. Yamaguchi, Nat. Commun. **2**, 198 (2011).
[121] S. R. Sklan and J. C. Grossman, arXiv:1301.2807 (2013).
[122] K. Stannigel, P. Komar, S. J. M. Habraken, S. D. Bennett, M. D. Lukin, P. Zoller, and P. Rabl, Phys. Rev. Lett. **109**, 013603 (2012).
[123] M. Schmidt, M. Ludwig, and F. Marquardt, New J. Phys. **14**, 125005 (2012).
[124] S. Rips and M. J. Hartmann, Phys. Rev. Lett. **110**, 120503 (2013).
[125] T. Faust, J. Rieger, M. J. Seitner, J. P. Kotthaus, and E. M. Weig, Nat. Phys. **9**, 485 (2013).
[126] H. Okamoto, A. Gourgout, C.-Y. Chang, K. Onomitsu, I. Mahboob, E. Y. Chang, and H. Yamaguchi, Nat. Phys. **9**, 480 (2013).
[127] Ö. O. Soykal, R. Ruskov, and C. Tahan, Phys. Rev. Lett. **107**, 235502 (2011).
[128] R. Ruskov and C. Tahan, Phys. Rev. B **88**, 064308 (2013).
[129] J. H. Cho, L. W. Weiss, C. D. Richards, D. F. Bahr, and R. F. Richards, J. Micromech. Microeng. **17**, S217 (2007).
[130] R. Martínez-Sala, C. Rubio, L. M. García-Raffi, J. V. Sánchez-Pérez, E. A. Sánchez-Pérez, and J. Llinares, J. Sound Vib. **291**, 100 (2006).